buildings

MDPI

*Article*

# Enhancing the Thermal and Energy Performance of Clay Bricks with Recycled Cultivated *Pleurotus florida* Waste

**Marwa Kamal Fahmy [1], M. M. Ahmed [2], Sally A. Ali [3], Dalia Tarek [4], Ibrahim M. Maafa [5,*], Ayman Yousef [5] and Ayman Ragab [6]**

1. Architecture Department, Faculty of Engineering-Mataria, Helwan University, Cairo 11718, Egypt; marwa_fakhry@m-eng.helwan.edu.eg
2. Mathematics and Physics Department, Faculty of Engineering-Mataria, Helwan University, Cairo 11718, Egypt; marwa_elnagar77@yahoo.com
3. Botany and Microbiology Department, Faculty of Science, Helwan University, Cairo 11795, Egypt; sally_ali@science.helwan.edu.eg
4. Department of Architecture Engineering, College of Engineering, Jazan University, Jazan 45142, Saudi Arabia; dhassan@jazanu.edu.sa
5. Department of Chemical Engineering, College of Engineering, Jazan University, Jazan 45142, Saudi Arabia; aymanhassan@jazanu.edu.sa or aymanyousef84@gmail.com
6. Department of Architectural Engineering, Faculty of Engineering, Aswan University, Aswan 81542, Egypt; ayman.ragab@aswu.edu.eg

* Correspondence: imoaafa@jazanu.edu.sa

**Abstract:** The development of energy-efficient and sustainable building materials is imperative to reduce energy consumption in the construction sector. This study addresses both the applied problem of increased solar heat gain and decreased indoor thermal comfort, as well as the scientific problem of reducing the thermal conductivity of clay bricks. It investigates the incorporation of recycled spent mushroom materials, consisting of *Pleurotus florida* mycelia and rice husk waste, as a novel additive in the production of fired clay bricks (FCBs) to enhance thermal insulation properties. The developed bricks were utilized in an optimized wall design for a residential building in New Cairo, Egypt. The wall design is created using energy modeling software, including Honeybee, Ladybug, Climate Studio, and Galapagos. The results demonstrate that an optimal waste content of 15% and a firing temperature of 900 °C yield the best thermal performance. Compared to traditional FCB walls, the new design incorporating the florida waste additive significantly improves thermal comfort, as indicated by a lower predicted mean vote and predicted percentage of dissatisfaction. Furthermore, the developed walls contribute to a reduction in $CO_2$ emissions of 6% and a decrease in total energy consumption of 38.8%. The incorporation of recycled florida waste offers a sustainable approach to enhancing standard brick fabrication processes. This work highlights the promise of agricultural waste valuation for the development of eco-friendly and energy-efficient building materials. Future research should explore the mechanical strength, acoustics, cost–benefit analysis, and field implementation of the developed walls, thereby addressing both the scientific and applied aspects of the problem.

**Keywords:** recycling; *Pleurotus florida* waste; energy efficiency; thermal insulation; building envelope; parametric optimization

check for updates

**Citation:** Fahmy, M.K.; Ahmed, M.M.; Ali, S.A.; Tarek, D.; Maafa, I.M.; Yousef, A.; Ragab, A. Enhancing the Thermal and Energy Performance of Clay Bricks with Recycled Cultivated *Pleurotus florida* Waste. *Buildings* **2024**, *14*, 736. https://doi.org/10.3390/buildings14030736

Academic Editors: Yanxue Li and Fanyue Qian

Received: 24 January 2024
Revised: 15 February 2024
Accepted: 25 February 2024
Published: 8 March 2024



## 1. Introduction

The urgency of mitigating energy consumption and improving thermal comfort in buildings has led to a growing emphasis on enhancing thermal performance [1]. The ASHRAE defines thermal comfort as the condition that represents environmental thermal satisfaction. It is susceptible to subjective evaluation. Two models are used to assess thermal comfort: the static model (PMV-PPD) and the adaptive model [2]. Fanger used the heat balance equations to produce the index (PMV and PPD) (Fanger 1970). According to the ASHRAE 55 standard, the thermal climate within a building must be comfortable for at least 80% of the users in order to be considered acceptable. PPD and PMV should both be between −0.5 and 0.5. PPD and PMV should be less than 10% [1,3] as seen in Figure 1. Material selection and manipulation are key factors in achieving energy efficiency goals [4–6]. The residential building sector, responsible for a substantial portion of energy consumption, primarily in heating and cooling, faces increasing pressure to adopt energy-efficient practices [7]. The associated rise in energy demand contributes to $CO_2$ emissions, climate change, and global warming, necessitating a shift towards sustainable building practices [8,9].

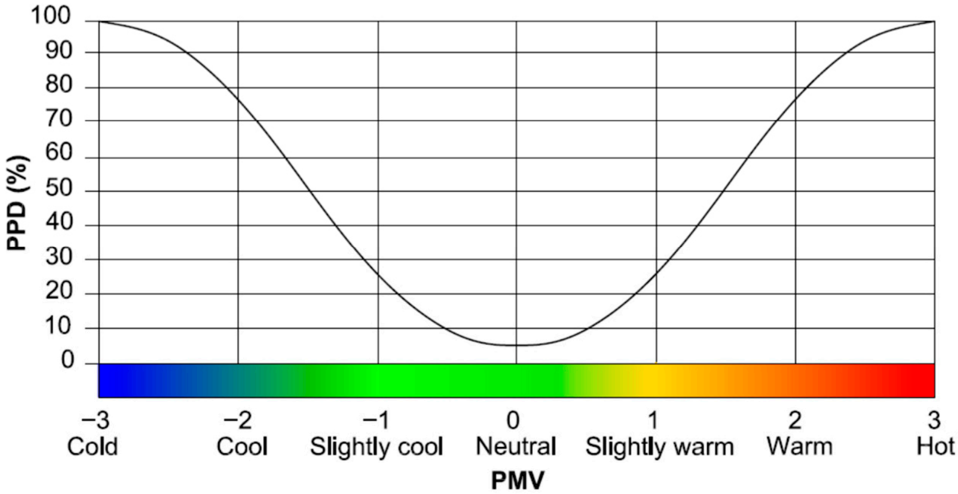


**Figure 1.** Predicted percentage dissatisfied PPD as a function of predicted mean vote (ASHRAE 55) [1].

In countries with hot climates like Egypt, improving building efficiency is of paramount importance [10–12]. Lightweight bricks have emerged as a critical component in high-performance thermal insulation, enabling effective energy management [13–17]. To further advance energy efficiency goals, it is essential to explore sustainable alternatives to traditional materials that offer comparable characteristics at reduced costs [18–23]. The utilization of waste-derived sustainable materials, such as recycled agricultural waste and stone wool waste, presents a promising avenue for enhancing thermal efficiency [13,24,25].

Several studies have focused on enhancing building thermal performance by optimizing wall sections, particularly in terms of wall layers [26–30]. The potential of agricultural waste as a source of sustainable building materials has gained significant research attention. One notable example explores the incorporation of pomegranate peel waste (PPW) into fired clay bricks to enhance their thermal properties and overall building performance [31,32]. Another study demonstrated that the combination of clay bricks with sludge and agricultural waste resulted in a 16.5% reduction in yearly energy consumption, accompanied by a 6.3% improvement in thermal comfort levels [25]. Another study utilized agricultural waste as a substitute for insulating materials in hollow bricks [33]. Additionally, research has highlighted various applications of agro-waste in building construction [34]. In a separate study, stone wool waste (SWW) generated from greenhouse agriculture was incorporated into brick manufacturing processes, thereby conserving natural clay resources and minimizing waste [24]. Previous studies have also employed building optimization techniques to enhance energy performance. These approaches primarily focused on walls and their features as key variables in the optimization process, aiming to improve thermal comfort through factors such as thermal conductivity, as well as to enhance heat gain through parametric design strategies [3,35].

The utilization of sustainable treated materials made from naturally occurring agricultural waste-recycling materials in building construction offers the potential for achieving carbon neutrality and reducing the positive carbon footprint associated with buildings [19]. Incorporating recycled agricultural waste, including secondary construction and demolition materials (SMMs), plays a critical role in this endeavor [36]. While factors such as building design, window specifications, and surrounding environments influence the reduction in energy consumption [1], employing sustainable and thermally isolated materials is considered the most effective parameter. Inefficient construction materials can contribute to excessive energy consumption throughout a building's lifespan, resulting in detrimental effects on the economy and the environment [37]. Thus, minimizing or avoiding thermal gains in buildings can yield advantages by improving user thermal comfort, reducing interior temperatures, decreasing the reliance on air conditioning systems, and lowering overall energy consumption.

The growing emphasis on a circular and sustainable economy has spurred interest in recycling SMMs, as exemplified by the proportion of SMMs disposed of in landfills, recycled for agricultural purposes, or incinerated in Malaysia [38]. To facilitate a sustainable energy transition, the development of fully biodegradable and eco-friendly thermal insulation materials becomes imperative. Mycelium-based materials harness the growth capabilities of fungi within lignocellulosic substrates, eliminating the need for synthetic binders and enabling the production of firm composite materials through substrate drying [39]. Research on mycelium-based composites includes the production of biodegradable packaging materials using Ganoderma fungal strains and processed cotton carpel and cotton seed hull [40], the production of biofoam using white-rot fungi-inoculated birch sawdust pulp [41], and the creation of mycelium bricks from rice husk waste employing fungal strains such as Oxyporus latermarginatus, Megasporoporia minor, and Ganoderma resinaceum [42]. The relatively low thermal conductivity of mycelium-based composites, typically around 0.05 W $m^{-1}\cdot K^{-1}$, positions them as promising materials for thermal insulation [43].

Rice husk, a significant waste product from rice production, presents an environmental challenge due to its non-humification nature [44]. However, it also holds promise as an organo-mineral raw material for mushroom cultivation, given its composition, which is rich in carbon and silicon [44]. The thermal conductivity of mycelium-based composites is influenced by the specific raw material and fungal strain used, leading to variations in thermal performance [40,43]. This characteristic is of economic significance, considering raw material costs and the disposal of SMMs [45,46]. Moreover, the incorporation of mycelium-based composites as thermal insulation offers a potential application for utilizing recycled SMMs and enhancing the sustainability of building materials [45].

To explore and optimize the thermal performance of wall designs, a parametric design approach can be employed. Parametric design is an algorithm-based method that permits the formulation of parameters and outcomes that, when combined, define, encode, and make clear the relationship between the design goal and the design response [47]. In general, in architectural design, any design elements, such as orientation, location, shape, envelope parameters, and so on, may be seen as what we refer to as "parameters". In the conventional method of design, the designer must go through the entire process again to modify any parameter once the basic model has been created. As a result, it is impossible to consider all viable design options and choose the best one. In this situation, parametric design is time-consuming. The only way to find several design options utilizing computational techniques in response to the challenges of architectural design is through parametric design [48,49]. The basis of the optimization method is parametric design. As the optimization engine receives an input from the users, it starts running and continues until it finds the best solution given the inputs [50]. This process needs a parametric platform such as Grasshopper.

The primary objective of this study is to recycle the waste of *Pleurotus florida* mushrooms to produce fired clay bricks and to examine the potential of these bricks to enhance thermal performance, reduce energy consumption, and contribute to the design of sustainable buildings. The utilization of mushroom biodegradation activities on rice husk waste aligns with zero-waste management policies and offers an environmentally friendly and cost-effective solution for brick manufacturing. The novelty of this research lies in its exploration of these objectives, which are crucial for advancing sustainable building practices. This study adopts a methodology that focuses on optimizing thermal performance and reducing energy consumption by utilizing the proposed materials. To facilitate this analysis, advanced software tools such as Rhinoceros 7 which include grasshopper are employed to calculate energy performance metrics. Furthermore, the genetic algorithm Galapagos is utilized to refine and optimize the parameters. The energy simulation conducted in this study encompasses various aspects, including thermal comfort, energy consumption measured in EUI (kWh/m$^2$), different energy loads, and $CO_2$ emissions.

## 2. Materials and Methods

The current research passed through different stages. The first stage of the study was the cultivation of *Pleurotus florida* (*P. florida*) on rice husk wastes, then preparation of their wastes for recycling in lightweight clay brick production. The first phase included the creation of brick samples with differing percentages of the cultivated *Pleurotus florida* wastes at a temperature of 900 °C, as depicted in Table 1. This stage also involved conducting the testing of the brick samples for their mechanical, physical, and thermal characteristics. In the present research article, two different raw materials were used, i.e., clay from the Aswan area in Upper Egypt and *Pleurotus florida* waste collected from drying mushroom spawn materials after cultivation of *Pleurotus florida* spawn using rice husk.

**Table 1.** Brick sample attributes.

| Samples | The Percentage of *P. florida* Wastes (%) | Firing Temperature °C |
|---|---|---|
| *P. florida* wastes—5% | 5 | |
| *P. florida* wastes—7.5% | 7.5 | |
| *P. florida* wastes—10% | 10 | 900 |
| *P. florida* wastes—12.5% | 12.5 | |
| *P. florida* wastes—15% | 15 | |

The second stage of the study involved determining the effective parametric variables, specifically the wall section and wall height. Subsequently, in the third stage, a thermal performance simulation was conducted to assess the potential thermal and energy performance of both traditional bricks and the proposed bricks in residential buildings located in New Cairo City. Moving on to the fourth stage, the envelope parameters were optimized using the Galagoes plugin to achieve the optimal design for the building envelope. Figure 2 illustrates the framework employed in this study.

### 2.1. Study Area

This study evaluates the thermal and energy performance benefits of clay bricks integrated with recycled *Pleurotus florida* waste in the context of a residential building located in New Cairo City, Egypt. Situated around 25 km east of Cairo in the Nile Delta region, New Cairo is a newly developed urban area founded in the late 20th century. Based on the climatic zone classification by the Housing and Building Research Center of Egypt, the city falls under the Delta and Cairo zones, characterized by a hot desert climate as depicted in Figure 3. Average temperatures range from 25 °C in January to 35 °C in July, with annual precipitation below 50 mm. Extreme heat and solar radiation necessitate building materials that minimize heat gain.

### 2.2. Materials and Fabrication Methods

#### 2.2.1. Raw Materials

The clay used as the primary ingredient in the manufactured bricks was analyzed using X-ray fluorescence (XRF) spectrometry, and the results confirmed the composition of the clay. The XRF of the raw materials are shown in Table 2. XRF analysis of the waste materials indicated a higher loss on ignition (LOI) due to their elevated organic content. X-ray diffraction (XRD) analysis further determined the main phases present in the clay and *P. florida*. Figure 4a displays the XRD pattern revealing that the clay mostly consists of $SiO_2$ and $Al_2O_3$. While *P. florida* comprises sodium aluminum silicate, davidsmithite, trinepheline, sodium aluminum silicate hydroxide, and wollastonite, as depicted in Figure 4b.

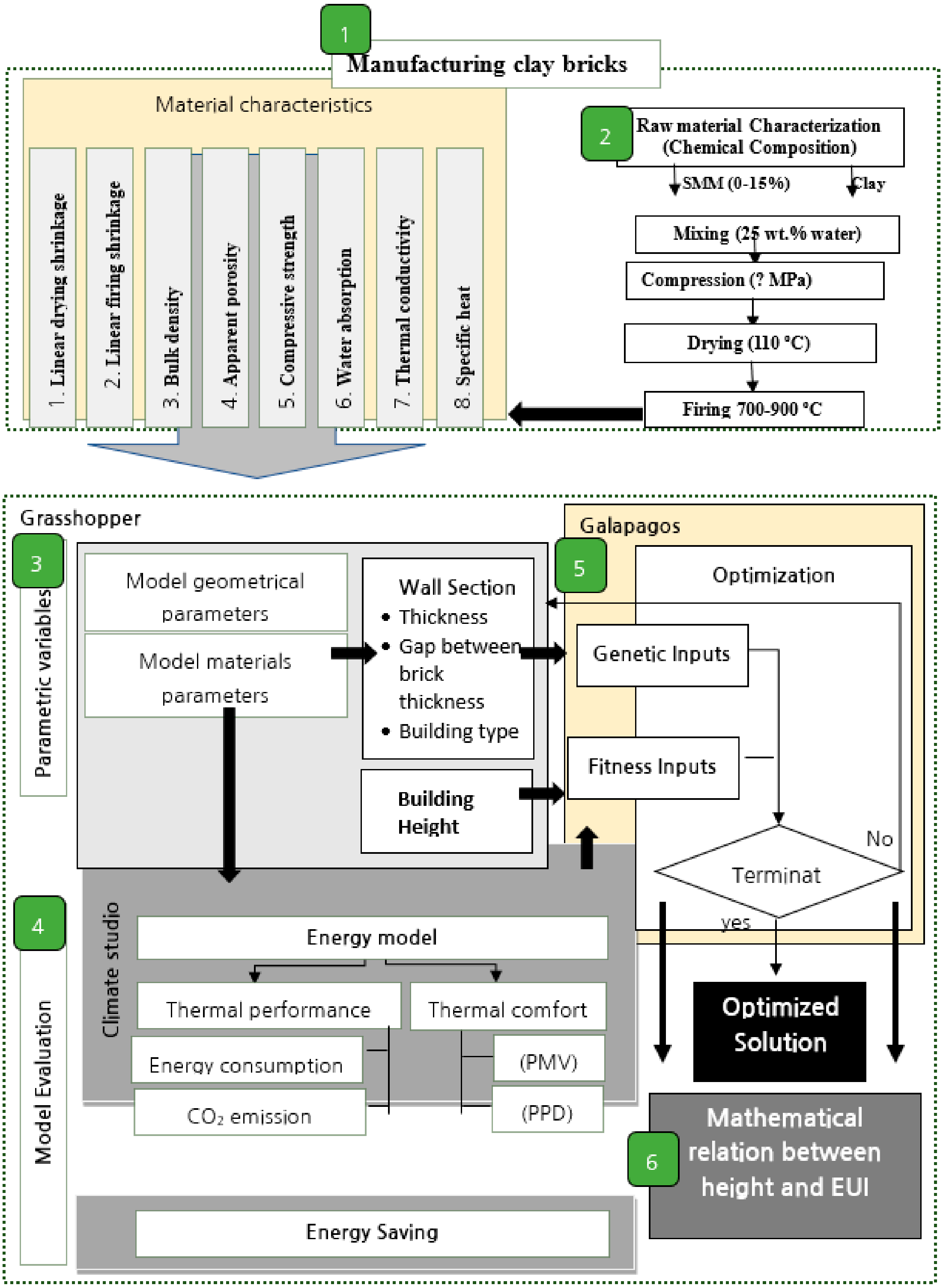


**Figure 2.** Study methodological farmwork.

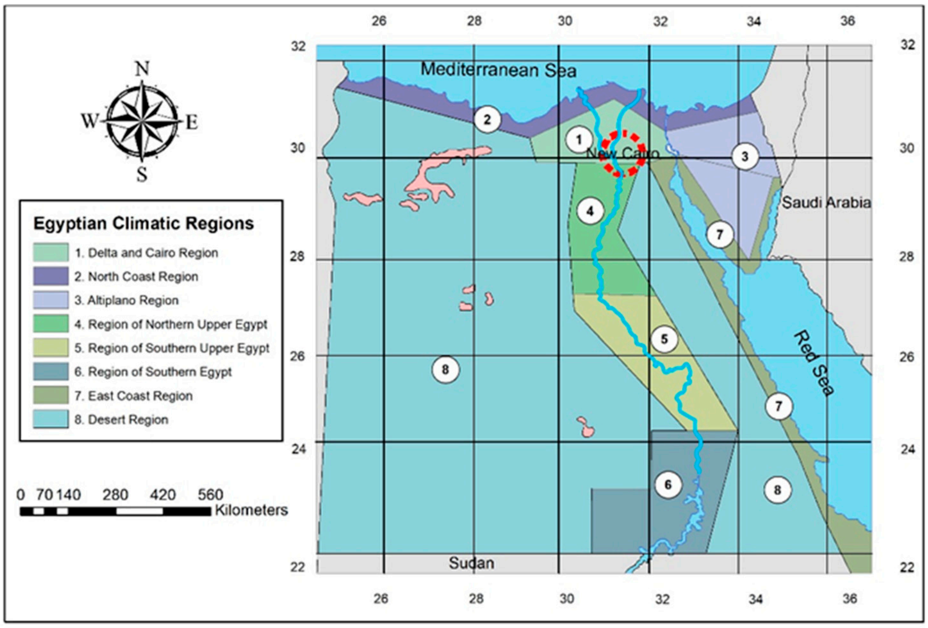


**Figure 3.** Location of New Cairo and the climatic regions.

**Table 2.** Chemical composition of raw materials.

| Composition | Clay wt. (%) | *P. florida* Wastes wt. (%) |
|---|---|---|
| $Al_2O_3$ | 32.906 | 0.07 |
| $SiO_2$ | 48.931 | 30.2 |
| $Na_2O$ | 0.094 | 0.38 |
| $K_2O$ | 0.014 | 0.66 |
| CaO | 0.505 | 1.58 |
| MgO | 0.09 | - |
| $TiO_2$ | 5.918 | - |
| $Fe_2O_3$ | 1.193 | 0.1 |
| $SO_3$ | 0.291 | - |
| F | - | - |
| Cl | 0.011 | - |
| $Cr_2O_3$ | 0.138 | - |
| $ZrO_2$ | 0.465 | - |
| LOI | 9.2 | 32 |
| TOTAL | 99.756 | 64.99 |

2.2.2. The Production of *P. florida* Wastes

In accordance with the procedures outlined by Okigbo et al. [51], with some modifications as depicted in Figure 5, the production of *Pleurotus florida* (*P. florida*) waste involved the cultivation of mycelial spawn within the rice husk substrate. The process commenced with the collection of mature *P. florida* fruiting bodies, which were grown on locally available agricultural wastes, specifically rice straws. The mushroom laboratory culture collection at the Agricultural Research Centre, Ministry of Agriculture, Giza, Egypt, provided the necessary grain spawns for the experiment.

To cultivate the *P. florida* mycelia, Potato Dextrose Agar (PDA) medium was prepared in sterile Petri dishes. Surface-sterilized mushroom samples were bisected longitudinally, and collar tissue sections from the cap–stalk junction were aseptically transferred onto the PDA plates. Under controlled conditions, the inoculated plates were incubated at 25 °C for one week to allow for the proliferation of *P. florida* mycelia. This tissue culture technique facilitated the isolation and subsequent inoculation of the mushroom mycelia into the agricultural waste substrate.

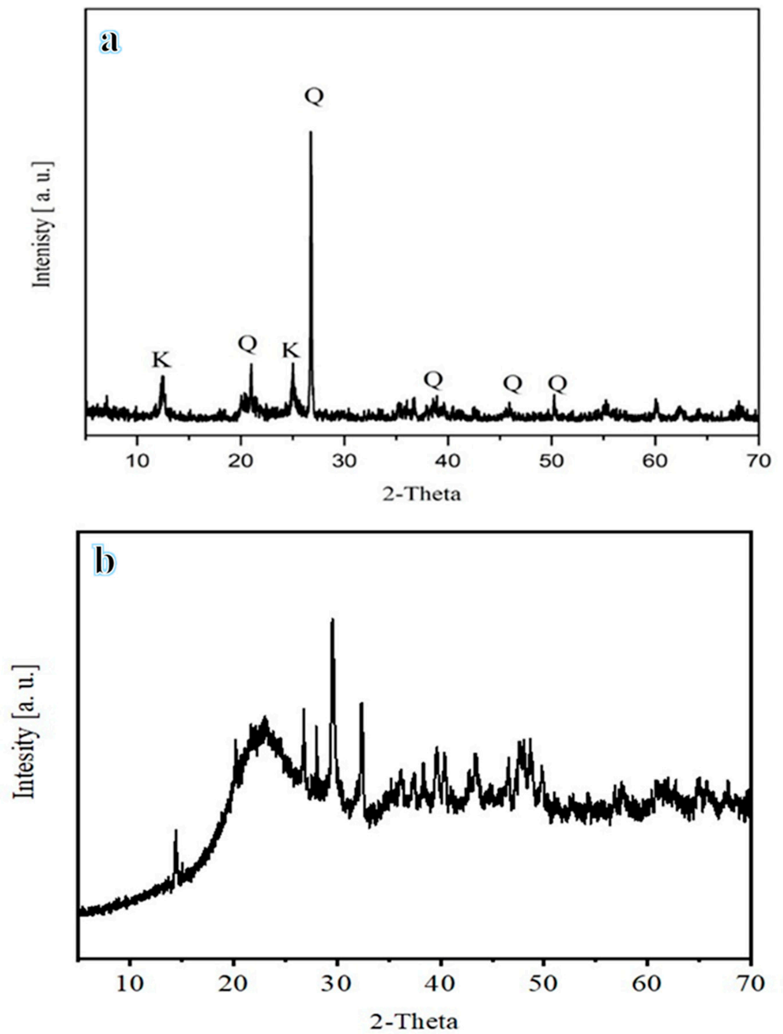


**Figure 4.** (**a**) XRD analysis of the clay, and (**b**) *P. florida* wastes.

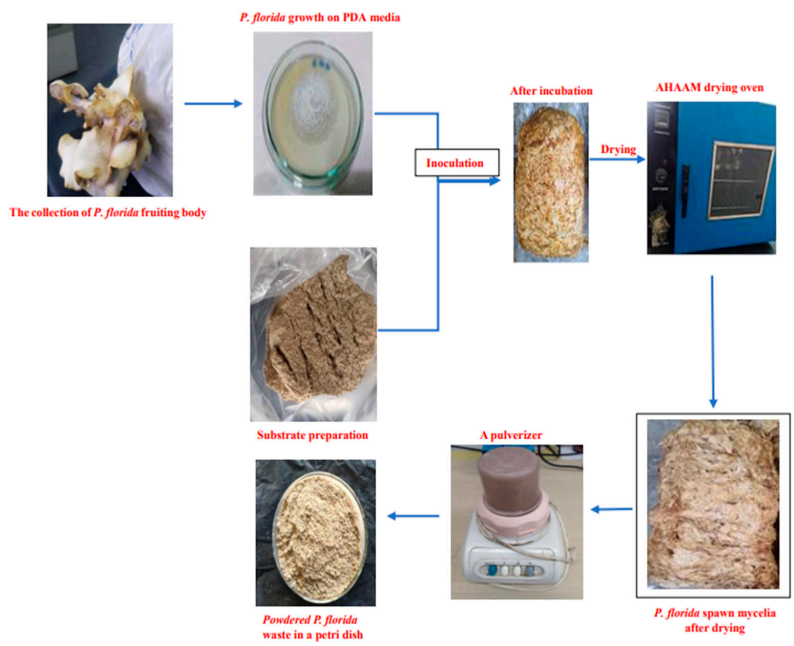


**Figure 5.** *Pleurotus florida* waste production steps.

The cultivation substrate consisted of rice husks obtained from a mill in El-Sharqhya, Egypt. The collected rice husk residue underwent a thorough rinsing with distilled water to eliminate any residual particulates. Subsequently, the rice husks were separated from the liquid by filtration through a 5 mm mesh and air-dried at ambient temperature. Further, the air-dried rice husks were oven-dried at 105 °C until a constant weight was achieved. This washing and drying pretreatment ensured the removal of impurities from the rice husks before steam sterilization and fungal inoculation.

Sterilized rice husk substrate bags were aseptically inoculated with 5 mm mycelial discs obtained from a 6-day culture of *Pleurotus florida*. The inoculated bags were carefully sealed to prevent contamination and incubated in dark conditions at 25 °C. Over a period of 15–20 days, the *P. florida* mycelia fully colonized the rice husk substrate within the bags. The incubation process was terminated by oven-drying the bags at 50 °C for 60 h, deactivating the mycelia and stabilizing the materials.

Upon harvesting the mushroom fruiting bodies, the remaining myceliated substrate bags were dried at 60 °C for 48 h. Subsequently, a mechanical grinder was employed to pulverize the dried bags, resulting in a powdered form. This powder was then sieved through a 2 mm mesh to eliminate impurities, yielding the spent *P. florida* material suitable for brick fabrication.

#### 2.2.3. Samples Preparation

The spent *P. florida* materials were incorporated into clay bricks at percentages of 0%, 5%, 7.5%, 10%, 12.5%, and 15% by weight. The clay and florida waste materials were finely mixed using a ball mill for 2 min to achieve a homogeneous dry blend. Water was added to prepare a paste containing 20% moisture content by weight. The mixtures were molded and compacted to remove air voids before being dried at 120 °C for 6 h. The dried samples were fired at 900 °C for 4 h at a heating rate of 10 °C/min to produce the final bricks.

### *2.3. Laboratory Characterization*

The fabricated bricks were subjected to the testing of key parameters including compressive strength, water absorption, density, apparent porosity, and thermal conductivity.

- Compressive Strength

The compressive strength was determined according to the ASTM C62 standards using a mechanical testing machine [19].

- Water Absorption, Density, and Porosity

Water absorption, bulk density, and apparent porosity were evaluated following the ASTM C62 guidelines [52]. Absorption indicates pore volume, density correlates with thermal conductivity [53], and porosity is linked to insulation capacity [54].

- Thermal Conductivity

The thermal conductivity was measured at room temperature using a KD2 Pro analyzer based on the transient heat conduction method according to the ASTM D5334 standards [55]. Lower thermal conductivity demonstrates enhanced insulation properties.

### *2.4. Simulation Process*

The study framework shown describes the process in which the wall design is optimized for optimum energy performance. First, the model plan is built in Rhino7 and inserted into Grasshopper (GH). Then, the 3D model is made in Grasshopper. Then, the thermal model is scripted into Grasshopper using ClimateStudio, Honeybee, and Ladybug (Grasshopper plugins). The plugins are engines for EnergyPlus, Radiance, and OpenStudio which simulate building energy and thermal comfort performance [50]. The materials are identified and added to the model as exterior wall materials. Then, we identified the input variations and their ranges in our case, as we focused on the impact of the wall design, the parameters such as wall thickness, wall design, and height became changeable parameters in our model and were added to Galapagos as input variations. The fitness inputs were the thermal performance. Afterward, two stages of optimization were run and the optimum solution was reached [56]. Finally, the relationship between the wall height and EUI was calculated, and a mathematical model was built.

The model was built in Rhinoceros 7 and inserted into Grasshopper as parametric software called a visual programming language. Ladybug (https://www.ladybug.tools/, accessed on 27 December 2023) is a Grasshopper plug-in that connects Grasshopper to engines such as EnergyPlus and Radiance (https://www.radiance-online.org/, accessed on 27 December 2023). These plugins transmit the model parameters as the input of simulation tools [50,57]. Grasshopper was applied to control the geometrical parameters of the model and the material properties. Sequentially, the Ladybug and Honeybee plug-ins were utilized to insert the physical properties of envelopes and to operate EnergyPlus as the energy simulation software. The study optimized the best wall section. The optimization processes were run on the Grasshopper plugin as depicted in Figure 6. Each brick with a different waste ratio was applied for each wall section and differentiated to the base case. Figure 7 shows the definition made in Grasshopper. The simulation includes four stages: (1) the thermal comfort index PPD and PMV, was simulated using Climate Studio; (2) energy consumption including the EUI, heating and cooling loads, and energy balance for each room was simulated using Climate Studio, using Honeybee and Ladybug; (3) the $CO_2$ emission and enhancement rate was simulated using Climate Studio; (4) the energy saving was optimized. In order to conduct the simulation for the study area, an EPW file was incorporated into the Grasshopper definition. An EPW file is a type of weather data file that encompasses typical meteorological data for a specific location and is utilized for building performance simulation purposes. The EPW file necessary for this study was obtained from climate.onebuilding.org, accessed on 27 December 2023, a platform that offers access to a wide range of EPW files for more than 16,100 locations globally, including Cairo. The website provides links to download EPW files from the EnergyPlus website, which are derived from the TMY2 dataset. These stages are described as the following:

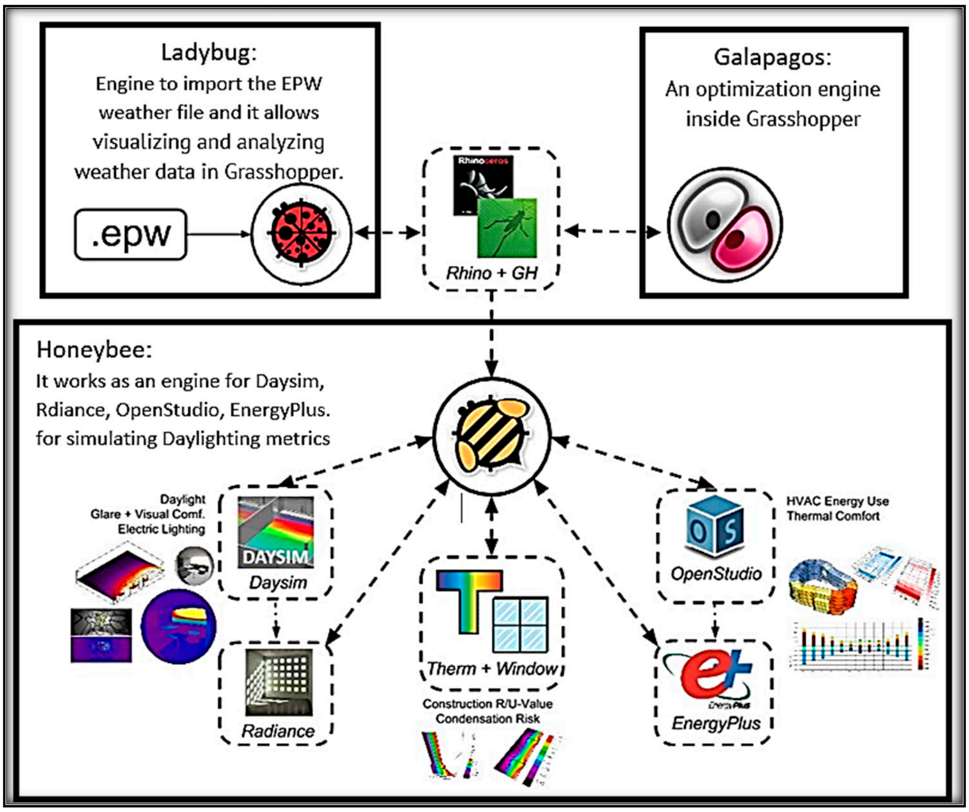


**Figure 6.** Schematic diagram for software used to support environmental design.

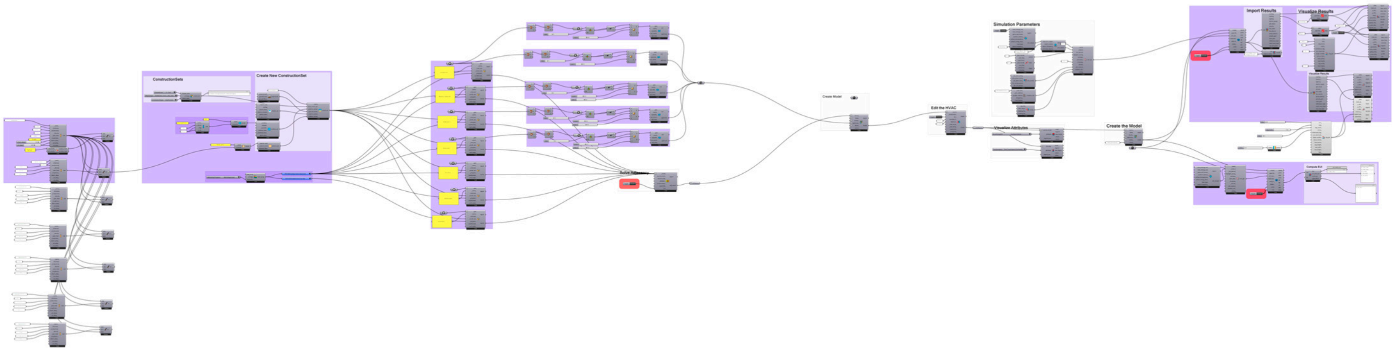

**Figure 7.** Definition made in Grasshopper.

2.4.1. Description of the Model (Case Study)

The case study focuses on a representative high-rise social housing building situated in New Cairo. The building comprises six above-ground floors and features four apartments per floor, each with a distinct orientation. To analyze the thermal performance, the study concentrates on simulating the southwest apartment, as it is anticipated to experience the highest heat gain. The detailed characteristics of the investigated building are presented in Figures 8 and 9.


(**a**) (**b**)

**Figure 8.** The investigated building: (**a**) 3D model of the case study, (**b**) plan and layout.

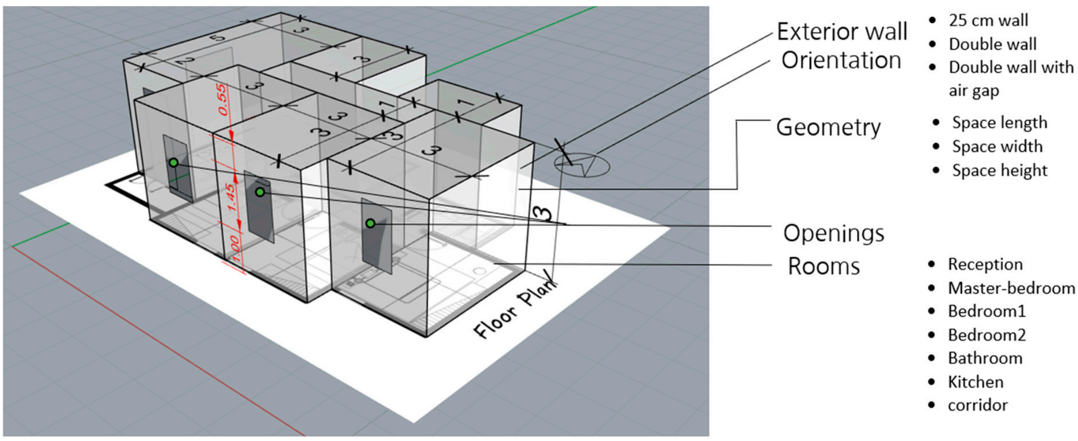


**Figure 9.** The case study description.

The floor-to-floor height of the building is 3.00 m, measured from finish to finish. The exterior walls are constructed with a thickness of 0.29 m and consist of three layers:

plaster on both sides with a brick layer in between. The apartment unit encompasses three rooms, and a bathroom, a kitchen, and a hall, with a total area of 90 square meters. The unit's layout allocates one room to the west, while the remaining rooms face south. For testing purposes, the unit is situated on the top floor, thereby subjecting it to the highest solar radiation levels within the building. EnergyPlus materials are employed for the construction of the building components.

Regarding the HVAC system, the Honeybee plugin serves as the computational engine for EnergyPlus. The air conditioning system is configured as an optimal load air system with a set temperature of 24 °C, to facilitate load calculations during the initial design stages. Given its residential nature, the building operates continuously throughout the day (24 h). Energy load simulations are conducted using Honeybee in conjunction with Daysim, Open Studio, and EnergyPlus. The evaluation incorporates metrics such as energy use intensity (EUI), heating and cooling loads, and energy balance. EUI is calculated as the annual energy consumption per unit of floor area (kWh/m$^2$) to enable effective comparisons between different materials. The primary objective is to minimize heating and cooling energy demand while simultaneously improving thermal comfort in each room, thereby reducing overall energy consumption.

#### 2.4.2. Thermal Performance and Optimization

For thermal performance, the research simulated two metrics: thermal comfort and energy consumption. The study measured two metrics for thermal comfort: PMV and PPD. It simulated the two indexes of thermal comfort for each wall section to optimize the wall section, determine the best-performed section, and then differentiate the results with the base case. Then, the study simulated the total EUI and energy balance. Finally, the study simulated the monthly heating and loads for the best wall section and base case.

Equations (1) and (2) were used to calculate the energy savings in the base case building by using the new wall section. For each optimum case, the study calculated the energy savings:

$$\text{Energy saving} = \text{Energy used (base—case)} - \text{energy used (using the new brick with waste ratio)} \quad (1)$$

$$\text{Energy saving \%} = \text{Energy saving/Energy used (base—case)}. \quad (2)$$

The optimization engine employed in this study is Galapagos, which plays a crucial role in enhancing energy efficiency by fine-tuning the design of a wall section. Galapagos achieves this by making adjustments to three key input parameters, referred to as "genomes": brick thickness, wall configuration (either single or double with an air gap), and the thickness of the gap in the double wall. The permissible range for brick thickness was set between 2 cm and 12.5 cm, while the gap thickness was constrained within the range of 0 cm to 12.5 cm. The different wall configurations were visually represented as a single wall (Figure 10A) and a double wall with an air gap (Figure 10B).

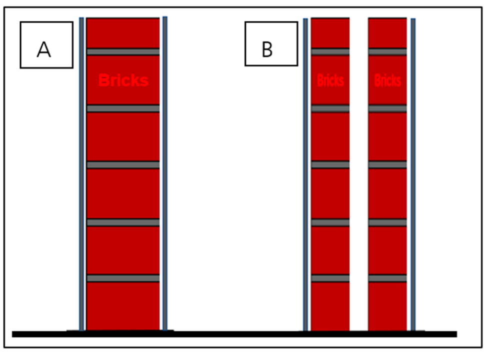


**Figure 10.** The wall section applied for optimizing wall design: (**A**) single wall, (**B**) double wall with air gap between them.

Operating as an optimization engine, Galapagos aims to minimize energy consumption and optimize energy use intensity (EUI) by iteratively adapting these input parameters. The optimization process, as depicted in Figure 11, involves defining an objective function that is directly linked to EUI. Additionally, constraints are imposed on the input parameters to ensure practicality and feasibility in real-world applications. Through this iterative exploration of various configurations and parameter adjustments, Galapagos refines the design of the wall section, ultimately striving for an energy-efficient outcome while adhering to the specified constraints.

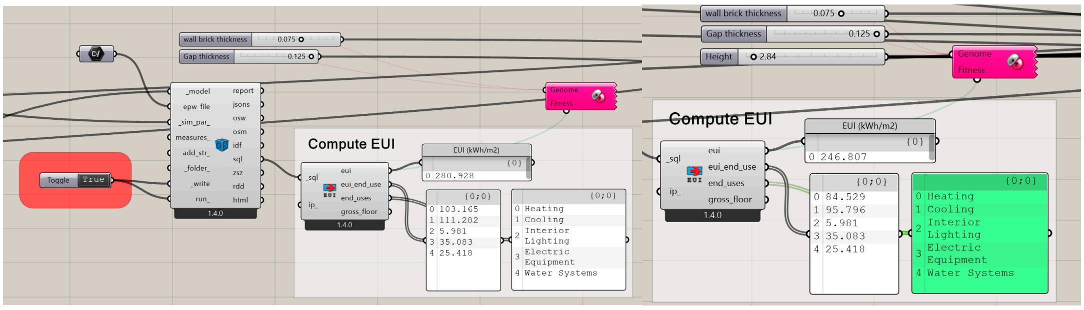

(**a**) (**b**)

**Figure 11.** The utilized engine for: (**a**) the wall section optimization, (**b**) building height optimization.

By utilizing Galapagos as the optimization engine in this study, the wall section design undergoes iterative refinement, allowing for the exploration of multiple configurations and parameter combinations. This approach aims to achieve an energy-efficient design while taking into account practical constraints. These refinements and optimizations enhance the clarity and comprehensibility of the research findings, facilitating a better understanding of the energy efficiency improvements achieved through the optimized wall section design.

Second, optimizing the building height with limitations between 280 cm and 350 cm. Third, building the mathematical relationship between height and the EUI.

## 3. Results and Discussion

The study results are structured into four primary sections. The first section examines the mechanical characteristics of the manufactured brick, including a comparative analysis to determine compliance percentages with the applicable Egyptian code. The second section investigates the physical properties of the manufactured brick samples. In the third section, data regarding the thermal conductivity of the fabricated brick are provided. This section also presents the outcomes derived from the simulation process, encompassing the internal thermal performance of the analyzed building, cooling energy consumption, and associated $CO_2$ emissions. The fourth section focuses on the optimization of wall design to attain an optimal energy use intensity. Finally, to generalize the findings to similar climatic regions, the study extended its application by utilizing the fabricated clay bricks in Jazan City, another city with comparable climatic conditions. By implementing the bricks in a different location, the study aimed to assess the transferability of the obtained results and their applicability in regions with similar environmental characteristics.

### *3.1. Mechanical Properties*

#### 3.1.1. Compressive Strength

The fabricated lightweight fired bricks were subjected to compressive strength testing, and the results are presented in Figure 12. Incorporating *P. florida* wastes in the burnt clay at a temperature of 900 °C resulted in a reduction in compressive strength from MPa to 18.8, 14.6, 10, 9.5, and 8 MPa for 5% *P. florida* waste, 7.5% *P. florida* waste, 10% *P. florida* waste, 12.5% *P. florida* waste, and 15% *P. florida* waste, respectively. This decrease in strength can be attributed to the formation of pores during the combustion of *P. florida* waste. The compressive strength values obtained for the fabricated bricks in this study were found to be within the range of 8 to 18.8 MPa, which is typically suitable for engineering applications [58]. Moreover, all the fabricated bricks complied with various international building standards, such as the ASTM C62-13a, 2013 [59], Brazilian Standard NBR 6064 (ABNT, 1983a) [60], Indian Standard (IS 1077, 2007) [61], Chinese National Standard (CNS 382:R2002, 2007) [62], and Egyptian Standard (ES4763/2006) [63].

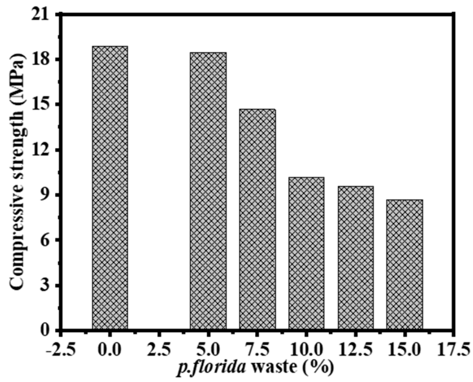


**Figure 12.** The compressive strength of fabricated fired bricks incorporated with different percentages of *P. florida* waste.

### 3.1.2. Water Absorption

The water absorption and porosity characteristics of lightweight bricks fired at 900 °C, with clay substitution ratios ranging from 0% to 15% of *P. florida* waste, are illustrated in Figure 13a. These parameters serve as indicators of brick durability and can provide insights into the material composition of the brick surface. The water absorption and porosity values exhibit an increase with higher proportions of *P. florida* waste, indicating its effectiveness as a pore-forming agent. Specifically, the incorporation of *P. florida* waste at ratios of 5%, 7.5%, 10%, 12.5%, and 15% resulted in water absorption values of 15%, 17%, 20%, 22.6%, and 23%, respectively, compared to 13.9% for *P. florida* waste at a ratio of 0%. The observed relationship between porosity and water absorption is consistent with Figure 13b. Porosity plays a crucial role in determining the physical and mechanical properties of bricks, with higher porosity favoring better insulation properties, where the compressive strength and density are reduced with increases in the porosity (Figure 13c). The maximum water absorption recorded was 23.5% for a *P. florida* waste ratio of 15%. Notably, this aligns with the water absorption limits specified for the moderate and normal weathering of clay building bricks in ASTM C62, where the maximum values are 22% and unlimited, respectively [64].

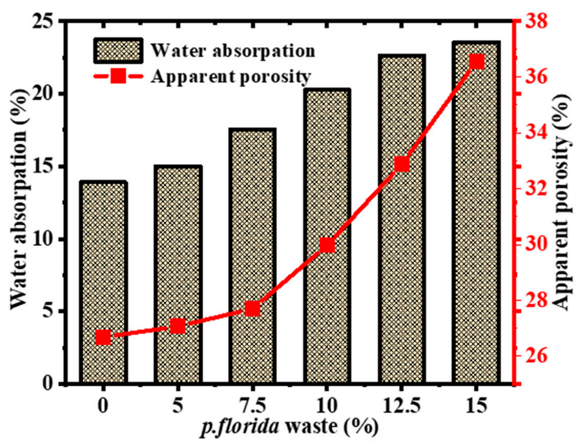


**Figure 13.** *Cont.*

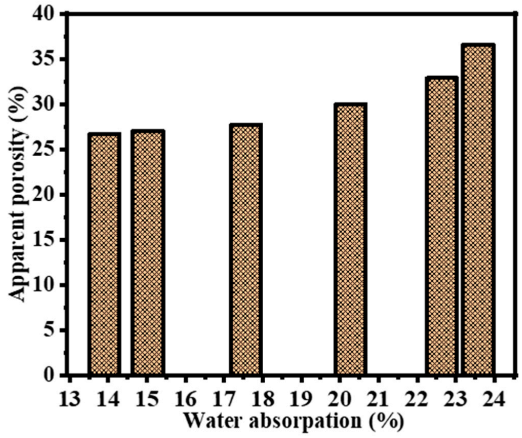


(**b**)

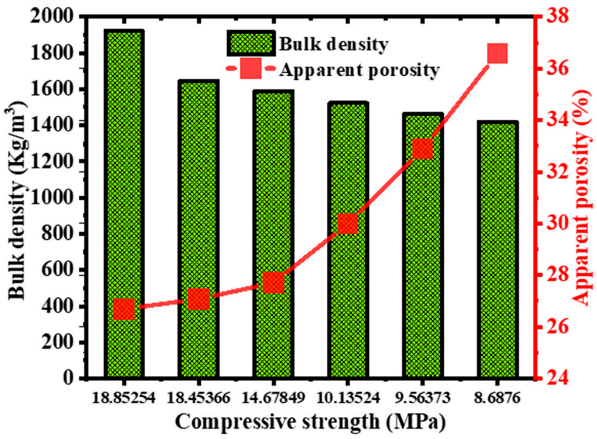


(**c**)

**Figure 13.** *P. florida* waste impacts on manufactured bricks: (**a**) Waste increases water absorption and porosity. (**b**) Water absorption relates directly to porosity. (**c**) Compressive strength and density decline as porosity rises.

## *3.2. Physical Properties*

### 3.2.1. Bulk Density

This study examined the use of *P. florida* waste as a lightweight aggregate in brick production. The incorporation of increasing percentages of *P. florida* waste resulted in a decrease in the bulk density of the bricks (Figure 14a), likely due to the elimination of organic materials and mineral hydrates or carbonates during firing, leading to increased porosity. The bulk density of the bricks fired at 900 °C consistently decreased with increasing percentages of *P. florida* waste, declining from 1922 kg/m$^3$ at 0% to 1419 kg/m$^3$ at 15%. The lower density indicates a higher porosity resulting from the evolution of volatile organic compounds and the combustion of biomass during the firing process.

As per the ASTM C90 standards [65], bricks with bulk densities below 1680 kg/m$^3$ are considered lightweight. An inverse relationship was observed between *P. florida* waste percentage and both bulk density and compressive strength (Figure 14b).

### 3.2.2. Apparent Porosity

The apparent porosity of the fired-brick samples was investigated through tests conducted at a temperature of 900 °C. The samples were prepared with varying percentages (0% to 15%) of *Pleurotus florida* waste as a replacement for clay. The results revealed that the brick samples containing florida waste exhibited higher porosity compared to the control samples at 900 °C. This can be attributed to the release of evolved gases during the decomposition of carbonaceous materials present in the florida waste. Additionally, the florida waste had a higher loss on ignition (LOI) compared to clay, further contributing to increased porosity [66].

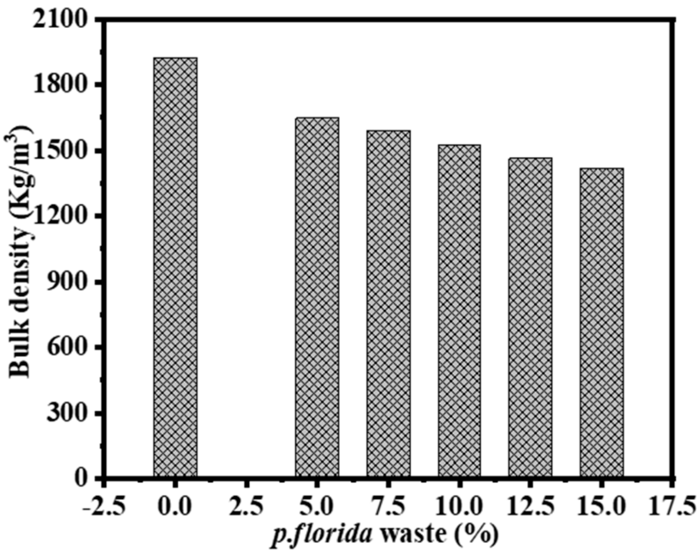


(**a**)

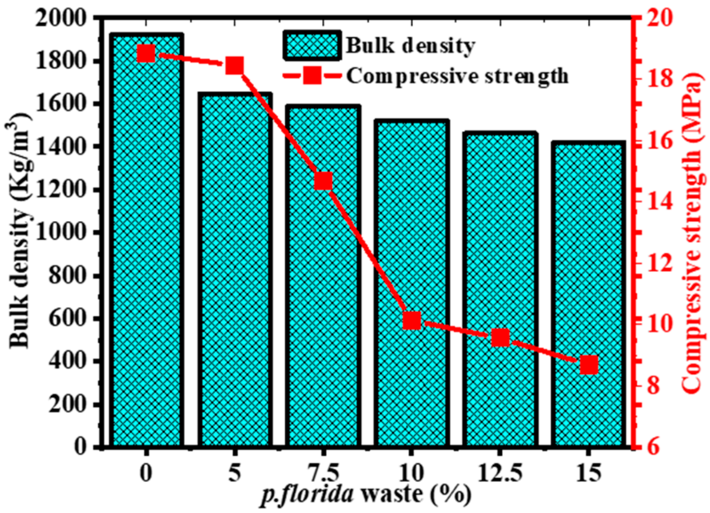


(**b**)

**Figure 14.** Effect of *P. florida* waste on brick bulk density: (**a**) Density declines linearly with waste percentage. (**b**) Compressive strength decreases as density reduces with more waste.

According to previous research by Sutcu and Akkurt [67], a porosity increases of more than 50% is considered effective in enhancing the insulation properties of fired clay bricks. In this study, the total porosity demonstrated an almost linear relationship with the increase in florida waste percentages, highlighting the effectiveness of florida waste as a pore-forming agent. Specifically, when substituting clay with 15 wt% florida waste at 900 °C, the porosity increased by approximately 36.6%. It is important to mention that the introduction of pores in the brick structure leads to a decrease in compressive strength, higher water absorption, and overall porosity. However, the increased porosity can have positive implications for brick performance, particularly in humid climate zones. The presence of pores facilitates the movement of water vapor within the brick structure, preventing the propagation of cracks [68].

### *3.3. Thermal Performance*

This study aimed to assess the thermal performance of clay bricks incorporating *Pleurotus florida* waste by examining their thermal conductivity and other relevant thermal properties. Two types of simulations were conducted to evaluate the impact of waste ratios in brick materials: thermal comfort and energy consumption. For thermal comfort analysis, the simulations focused on predicting the PMV and PPD values. On the other hand, energy consumption was evaluated through simulations of EUI, heating and cooling loads, and energy balance.

#### 3.3.1. Thermal Conductivity

The addition of *P. florida* waste as a pore-forming additive in brick production led to a gradual reduction in thermal conductivity as the percentage of waste increased from 0% to 15%, as shown in Table 3. All the brick formulations exhibited lower thermal conductivity values compared to conventional bricks, indicating their potential for use in energy-efficient building construction. A strong linear correlation was observed between thermal conductivity, porosity, and density, as depicted in Figure 15a. The thermal conductivity demonstrated a significant inverse correlation with both porosity and bulk density. Specifically, the thermal conductivity decreased from 0.77 W/m·K for conventional bricks to 0.293 W/m·K for bricks containing 15% *P. florida* waste. This decrease can be attributed to the increased pore volume and the disruption of heat transfer pathways within the brick matrix caused by the incorporation of the organic waste additive.

**Table 3.** Thermal conductivity for each investigated sample.

| ***P. florida* Waste (%)** | **Thermal Cond. (W/m·K)** | **Specific Heat (MJ/m$^3$·K)** | **Density (Kg/m$^3$)** |
|---|---|---|---|
| 0 | 0.77 | 1.6 | 1922.027 |
| 5 | 0.481 | 1.513 | 1646.172 |
| 7.5 | 0.43 | 1.433 | 1589.453 |
| 10 | 0.379 | 1.407 | 1523.376 |
| 12.5 | 0.327 | 1.367 | 1462.963 |
| 15 | 0.293 | 1.307 | 1419.981 |

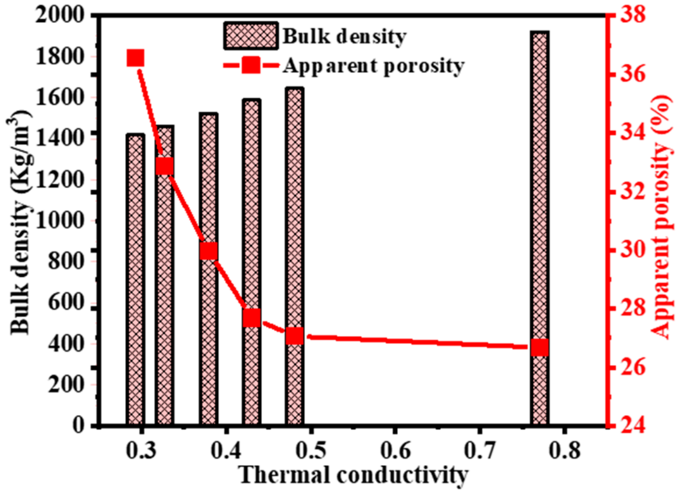


(**a**)

**Figure 15.** *Cont.*

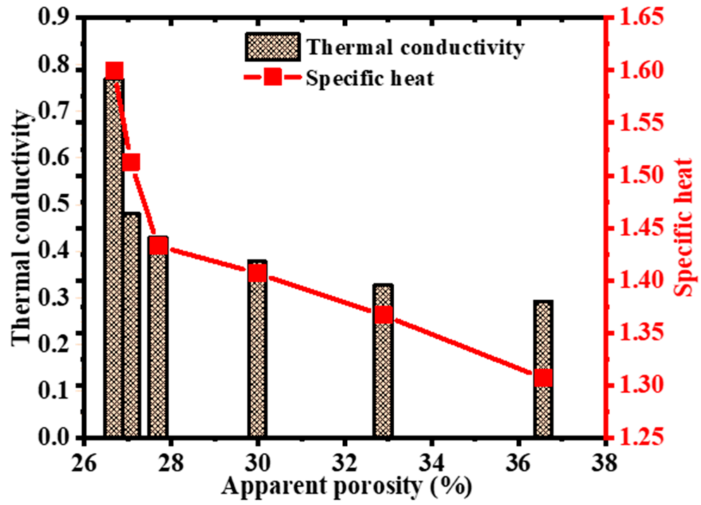


(**b**)

**Figure 15.** *P. florida* waste impacts on brick thermal performance: (**a**) Lower density decreases thermal conductivity and porosity. (**b**) Porosity increase reduces thermal conductivity and specific heat.

The specific heat capacity also exhibited a declining trend with increasing percentages of *P. florida* waste. This phenomenon can be attributed to the lower specific heat of the air present within the pores compared to that of the brick materials. However, the reduction in specific heat capacity was less significant compared to the decrease in thermal conductivity. The relationship between thermal conductivity, apparent porosity, and specific heat is depicted in (Figure 15b). The progressive increase in porosity and the associated improvements in thermal insulation properties with the addition of *P. florida* waste highlight its effectiveness as a sustainable pore-forming material for energy-efficient brick manufacturing. By optimizing the composition of the bricks and the firing conditions, it may be possible to produce building materials with thermal conductivities below 0.25 W/m·K, comparable to conventional insulating materials.

### 3.3.2. Thermal Comfort

The results for thermal comfort showed promising improvements in both PMV and PPD. The enhancement increases gradually by increasing the waste ratio in the bricks up to 15%. The simulation shows the best results for PMV and PPD by the additive of waste of 15%. The results presented in Table 4 signify significant advancements in thermal comfort, as measured by the Predicted Mean Vote (PMV) and Predicted Percentage of Dissatisfied (PPD). These findings are of paramount importance as they shed light on the influence of waste ratio in the brick material on indoor thermal conditions. The observation that "the enhancement increases gradually by increasing the waste ratio in the bricks up to 15%" is a pivotal revelation, indicating a proportional relationship between the waste ratio and improved thermal comfort, aligning with the principles of thermal insulation and energy efficiency. Notably, the simulation results pinpoint an optimal waste ratio of 15% as the point at which thermal comfort, as measured by PMV and PPD, reaches its peak performance. This specific threshold is significant, as it provides a clear directive for material selection in sustainable building design. Architects, engineers, and builders can utilize this insight to create structures that maximize thermal comfort while minimizing environmental impact. The analysis underscores a compelling trend—thermal comfort exhibits a gradual improvement as the waste ratio in the materials increases. This finding signifies a proportional relationship between waste ratio and enhanced thermal comfort, where a higher waste ratio contributes to superior insulation and reduced heat transfer. This deeper insight into the incremental improvement in thermal comfort enhances the study's relevance for sustainable construction practices and underscores the potential for architects and builders to optimize indoor thermal conditions effectively.

**Table 4.** Simulation results for PMV and PPD.

| Wastes (%) | | PMV | | PPD |
|---|---|---|---|---|
| 0 | 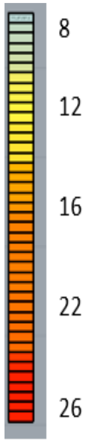 | 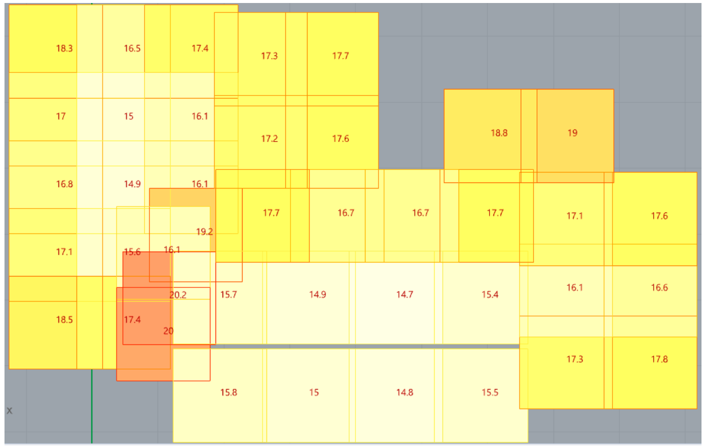 | 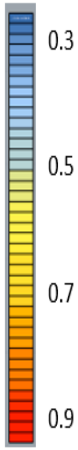 | 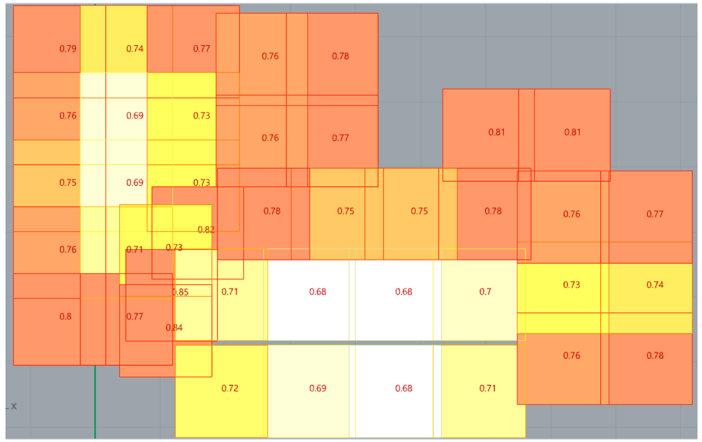 |
| 5 | | 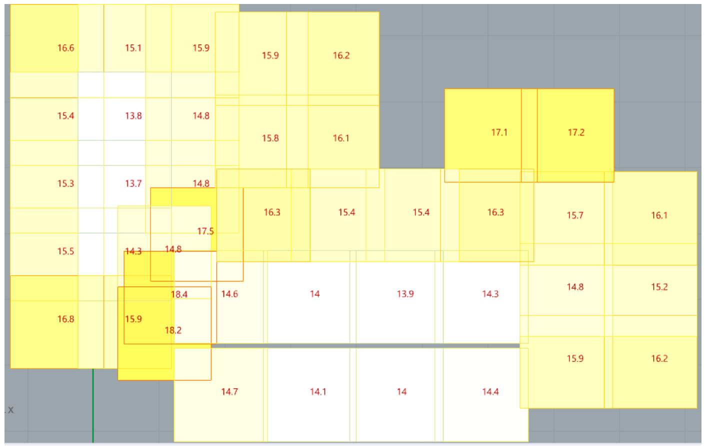 | | 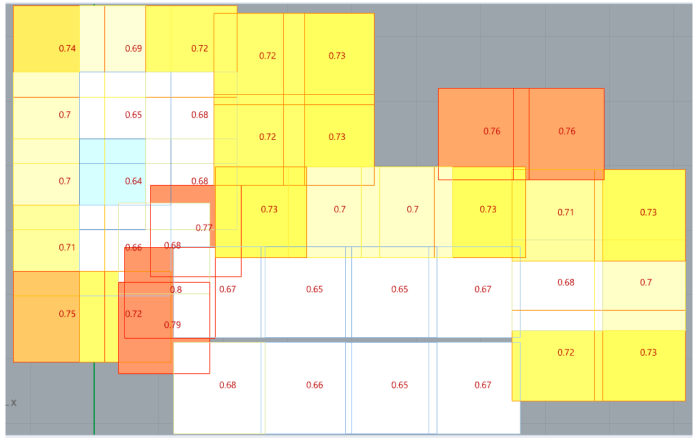 |

**Table 4.** *Cont.*

| Wastes (%) | PMV | PPD |
|---|---|---|
| 7.5 | 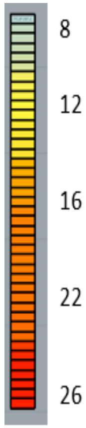 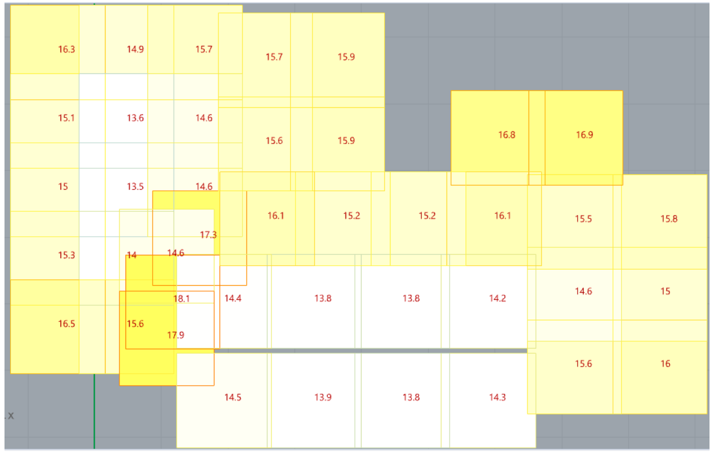 | 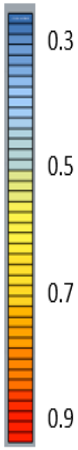 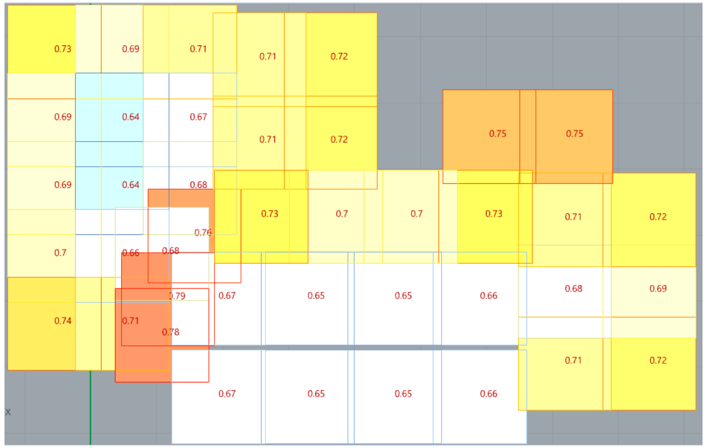 |
| 10 |  | 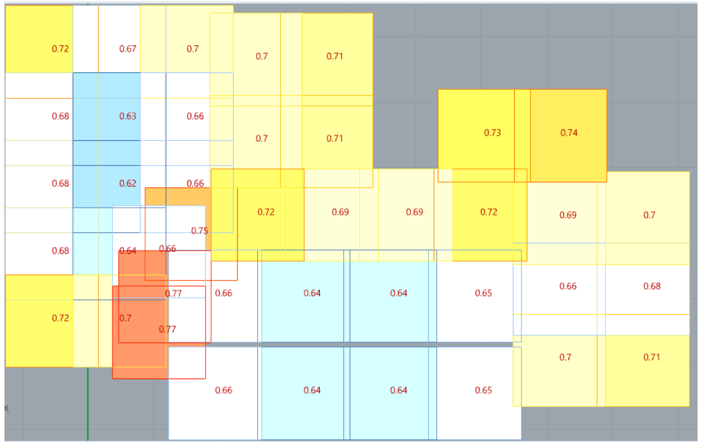 |

**Table 4.** *Cont.*

| Wastes (%) | PMV | | PPD | |
|---|---|---|---|---|
| 12.5 | 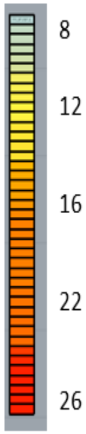  |  | 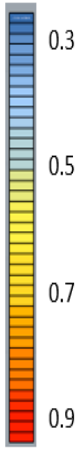  | 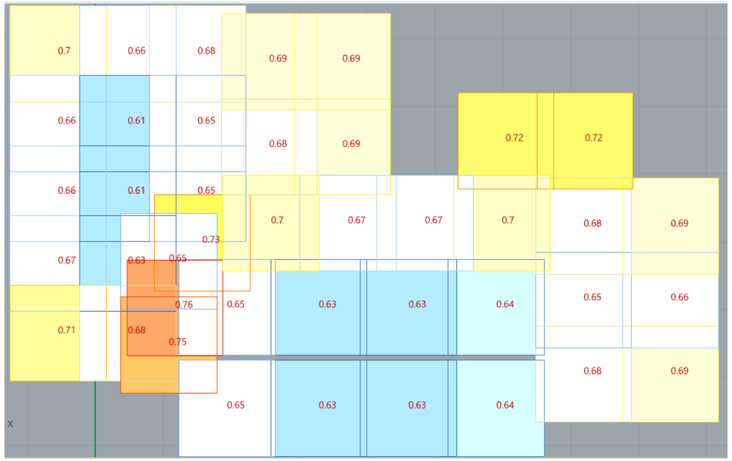 |
| 15 | | 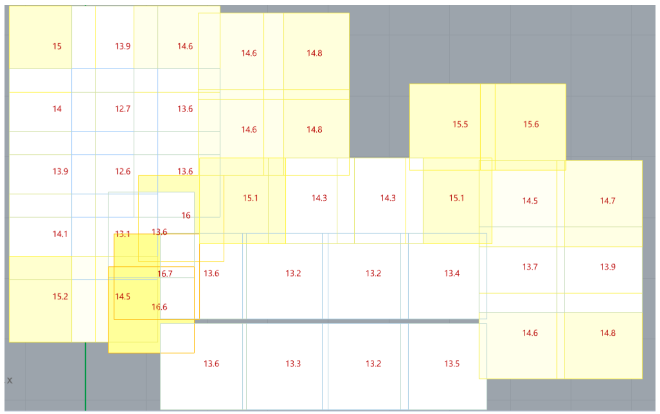 | | 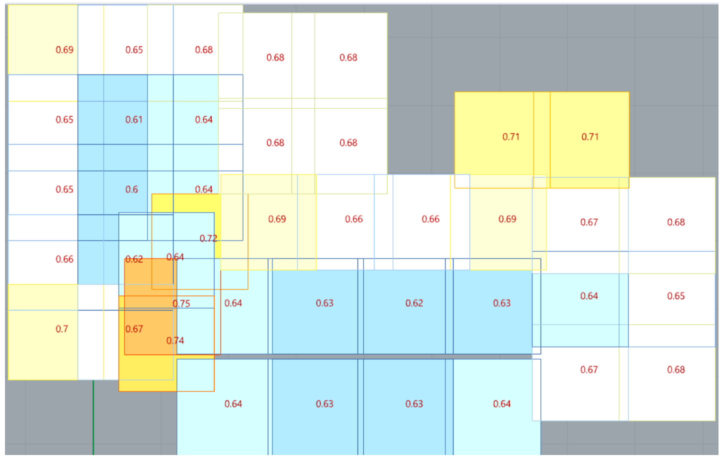 |

### 3.3.3. Energy Consumption

For energy consumption, the study simulates EUI bricks with each waste ratio. The study also simulates cooling and heating loads. Figure 16a–c show the results of the EUI, cooling, and heating loads. The waste ratio decreases the EUI values gradually. It also reduces the energy balance, cooling, and heating loads.

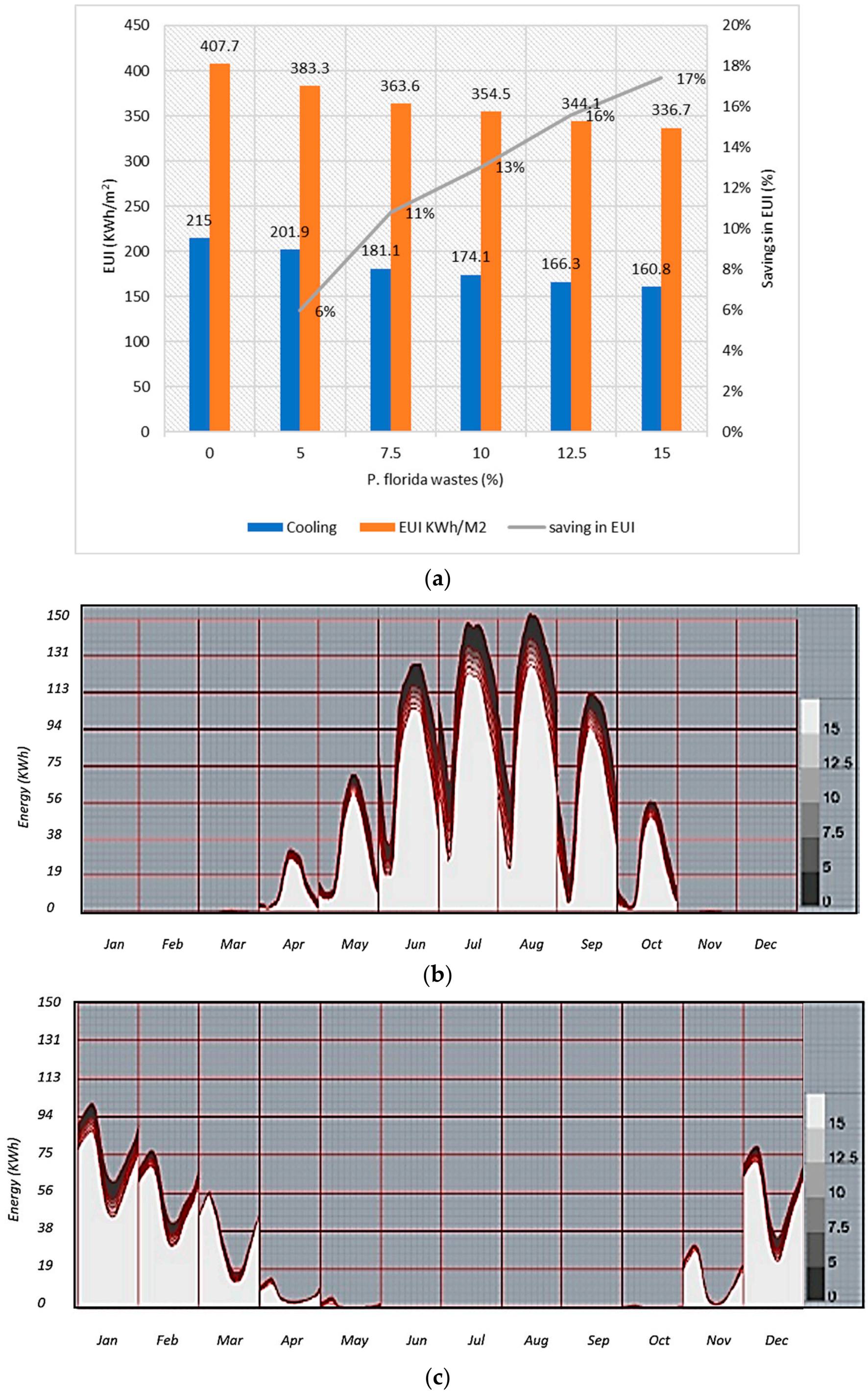


**Figure 16.** The results of: (**a**) the EUI, cooling, and heating loads, (**b**) monthly cooling, and (**c**) heating loads.

### 3.3.4. Best EUI Values

The results demonstrate that the waste ratio of 15% exhibited the best results, thus the study compares the energy balance and the cooling and heating loads for each room of the building by using bricks with a 15% waste ratio with the base case model. Table 5 presents the energy balance comparison. Table 6 shows the cooling and heating loads, respectively.

**Table 5.** Energy balance comparison between the base case and the bricks with 15% of waste.

| **Waste %** | **Energy Balance** | **Waste %** | **Energy Balance** |
|---|---|---|---|
| Legend bar | 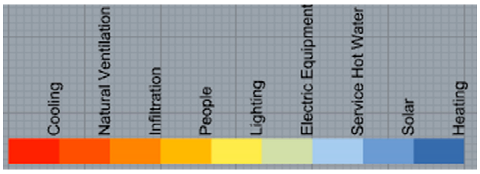 | | |
| 0% | 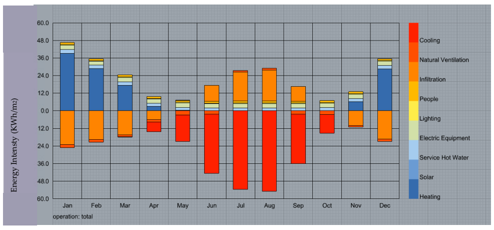 | 15% | 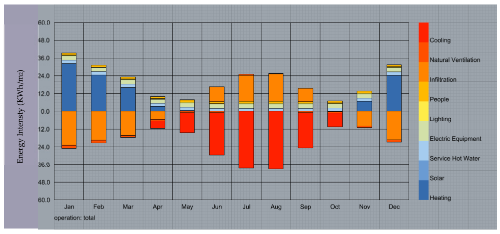 |

### 3.3.5. Decreased $CO_2$ Emissions

The bricks with the greatest waste ratio show the lowest $CO_2$ emissions. $CO_2$ has an inversely proportional relation to the waste ratio. For the 15% waste ratio, almost a 6% reduction in $CO_2$ emissions is achieved compared to the base case—see Figure 17 for the improvement rate in terms of $CO_2$ reduction.

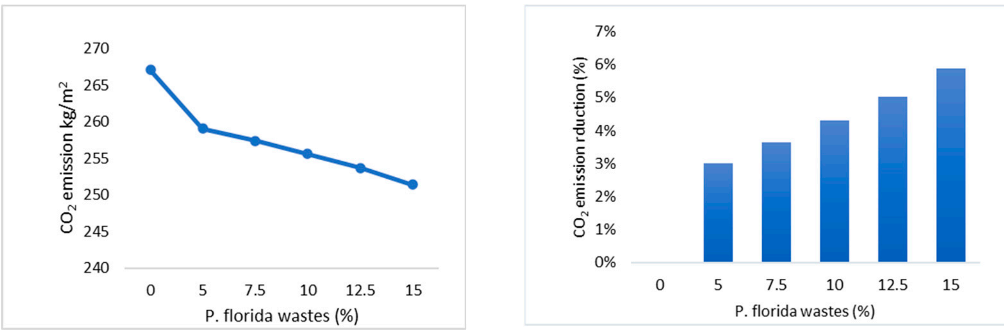


(**a**) (**b**)

**Figure 17.** $CO_2$ emissions: (**a**) the annual amount of $CO_2$ emissions, (**b**) the improvement rate in terms of $CO_2$ reduction.

### 3.3.6. Energy Saving

The building's performance was evaluated based on energy performance. By using Equations (1) and (2). The brick with a waste ratio of 5% saves 6%, and the results are improved gradually. Figure 18 shows the best energy saving of 17% by using bricks with 15% of waste. The incorporation of waste materials into brick production was investigated, resulting in energy savings of 6%, 11%, 13%, and 16% for waste percentages of 5%, 7.5%, 10%, and 12.5%, respectively.

**Table 6.** The cooling loads for each room of the apartment for the best waste ratio of 15% and the base case.

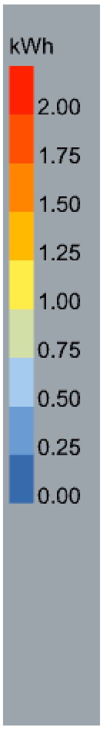


| | Cooling Loads Per Months | |
|---|---|---|
| | **Base Case Model** | **Waste 15%** |
| Bathroom | 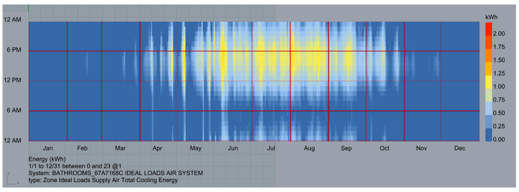 | 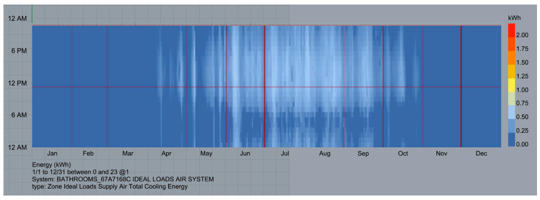 |
| Bedroom1 | 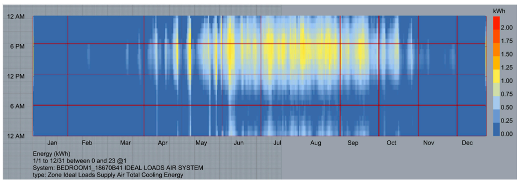 | 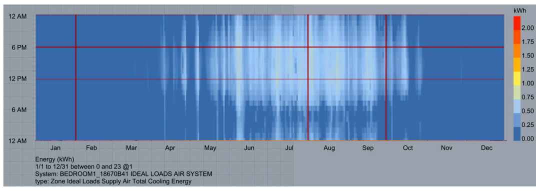 |
| Bedroom2 | 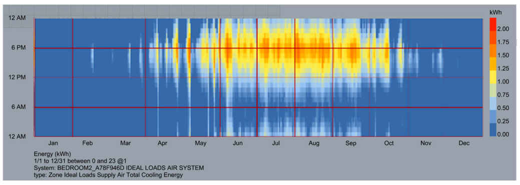 | 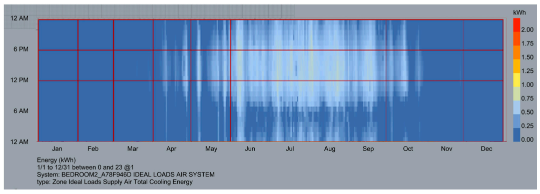 |
| Corridor | 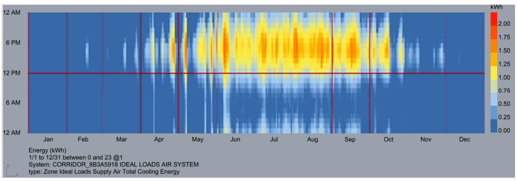 | 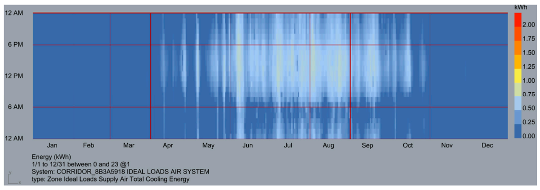 |
| Kitchen | 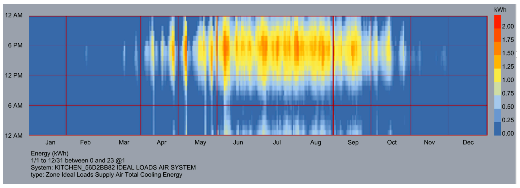 | 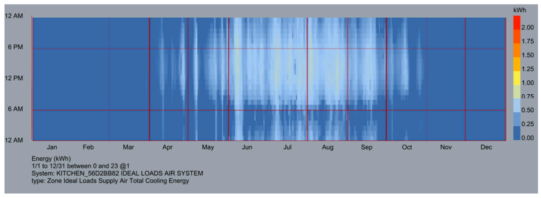 |
| master bedroom | 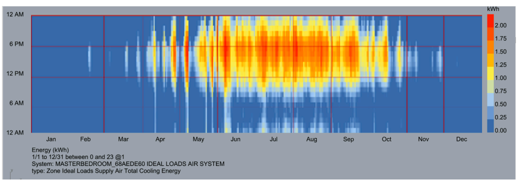 | 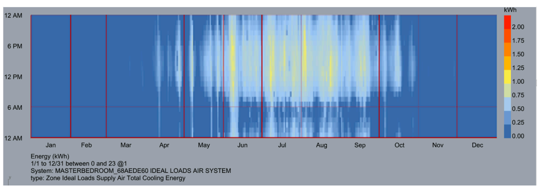 |
| Reception | 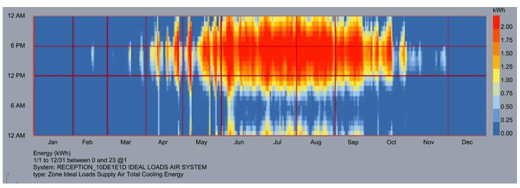 | 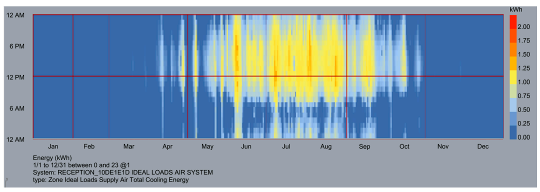 |

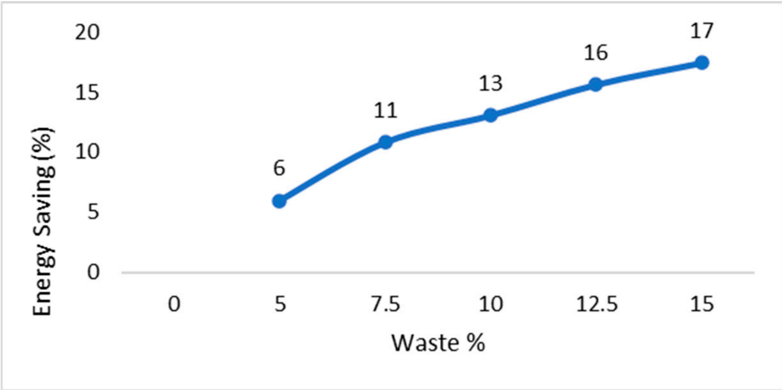


**Figure 18.** Energy saving by using each waste ratio.

## *3.4. Optimum Wall Design*

For the optimum wall design, the study optimizes the wall section. Then, the study optimizes the wall height with the wall section to investigate the impact of changing the wall height. Finally, the study builds a mathematical model to relate the wall height and EUI.

### 3.4.1. Wall Section Optimization

The optimization was run for six generations. We could find the optimum solution starting from the third generation. Figure 19 shows the optimization process. The results show that gap thickness has a greater effect than brick thickness. All the optimum results have greater gap thicknesses with different brick thicknesses. Cases 1, 4, 11, and 14 show the optimum wall section with maximum wall brick thickness and maximum gas thickness as shown in Table 7.

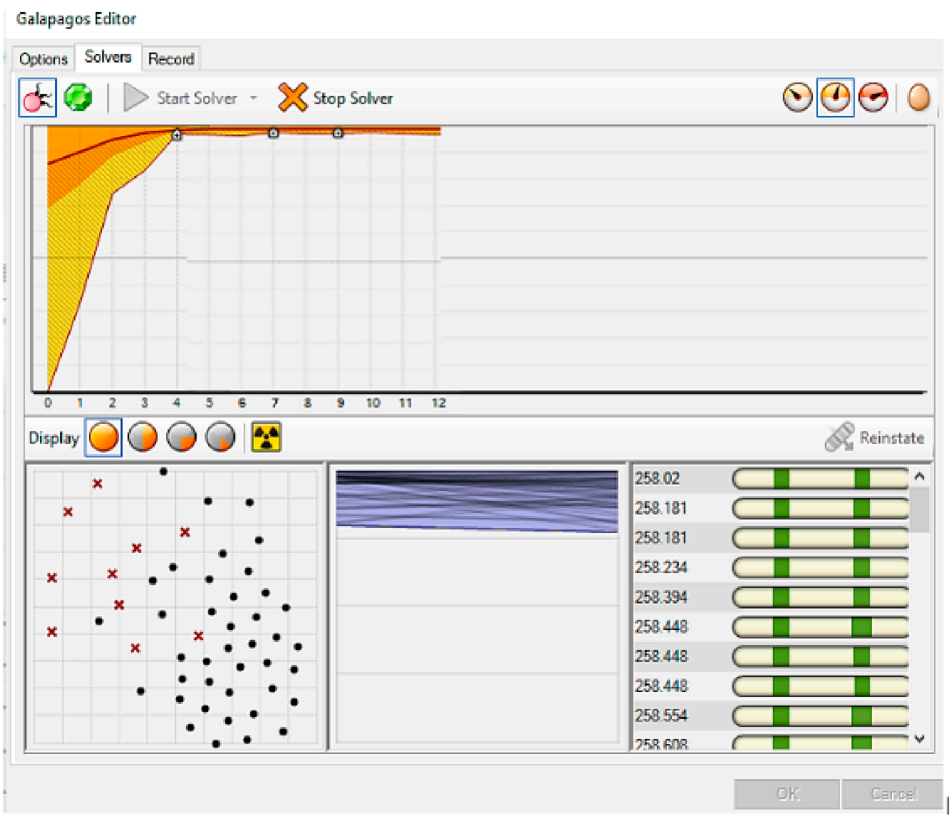


**Figure 19.** Optimization process for the wall section. × is deleted Genomes, • remaining Genomes.

**Table 7.** The table illustrates the outcomes of the optimization process for the wall section, aiming to achieve minimized energy usage intensity and maximal energy savings.

| | Case 1 | Case 2 | Case 3 | Case 4 | Case 5 | Case 6 | Case 7 | Case 8 | Case 9 | Case 10 | Case 11 | Case 12 | Case 13 | Case 14 | Case 15 |
|---|---|---|---|---|---|---|---|---|---|---|---|---|---|---|---|
| Brick Thickness in cm | 12.5 | 11.7 | 7.5 | 11.3 | 8.4 | 12.2 | 11.2 | 9.6 | 8.8 | 12.3 | 10.4 | 10 | 11.6 | 10.2 | 11.5 |
| Gap Spacing in cm | 12.5 | 12.3 | 12.5 | 12.1 | 12.5 | 12.5 | 11.5 | 11.3 | 12 | 11.4 | 11.5 | 12 | 12.4 | 12.2 | 12 |
| EUI In kWh/m$^2$ | 258.127 | 258.605 | 260.21 | 259.142 | 259.783 | 258.074 | 260.263 | 261.278 | 260.477 | 259.889 | 260.637 | 259.676 | 258.554 | 259.462 | 258.982 |
| Enhancement Ratio | 36.7% | 36.6% | 36.2% | 36.4% | 36.3% | 36.7% | 36.2% | 35.9% | 36.1% | 36.3% | 36.1% | 36.3% | 36.6% | 36.4% | 36.5% |

### 3.4.2. Wall Height Impact

In order to investigate the effect of wall height and to establish the mathematical relationship between the wall height EUI, the study applies the optimization process while adding the height to the solver genius. This process will help also in selecting the best wall design. Figure 20 and Table 8 show the optimization processes for the wall design including the wall height.

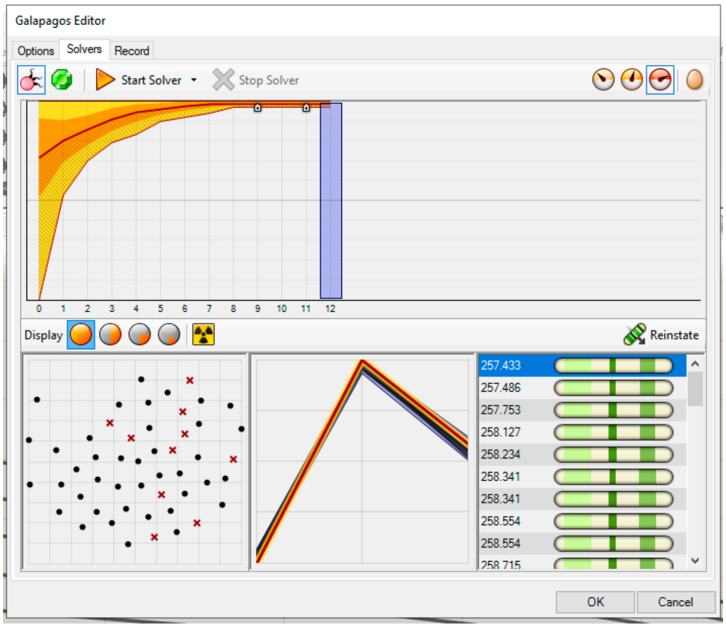


**Figure 20.** Optimization process for the wall design including the wall height. is deleted Genomes, remaining Genomes.

**Table 8.** Wall design optimization results: the height is added to the wall section. The green shaded column shows the optimum solution.

| | Case 16 | Case 17 | Case 18 | Case 19 | Case 20 | Case 21 | Case 22 | Case 23 | Case 24 | Case 25 | Case 26 |
|---|---|---|---|---|---|---|---|---|---|---|---|
| Brick Thickness, cm | 7.7 | 7.5 | 8 | 7 | 8 | 9.5 | 7.2 | 7.6 | 9 | 10 | 10 |
| Gap Spacing. cm | 12.5 | 12.5 | 12.5 | 12.5 | 12 | 11 | 12.5 | 12 | 12 | 11 | 11.5 |
| EUI, kWh/m$^2$ | 280 | 280 | 280 | 280 | 280 | 280 | 285 | 280 | 280 | 280 | 285 |
| Wall height | 249.477 | 249.53 | 249.317 | 249.744 | 250.171 | 251.239 | 249.637 | 250.331 | 249.69 | 251.025 | 252.841 |
| Enhancement ration | 38.8% | 38.8% | 38.8% | 38.7% | 38.5% | 38.4% | 38.8% | 38.6% | 38.8% | 38.4% | 38.0% |

### 3.4.3. Mathematical Relationship between Height and EUI

For a better understanding of the relationship between wall height and energy consumed in the building, the study simulated walls with different heights while fixing the wall thickness at 7.5 cm and gap thickness at 12.5 cm. The walls gradually increase in height, and the EUI for each one is simulated, as seen in Figure 21 and Table 9.

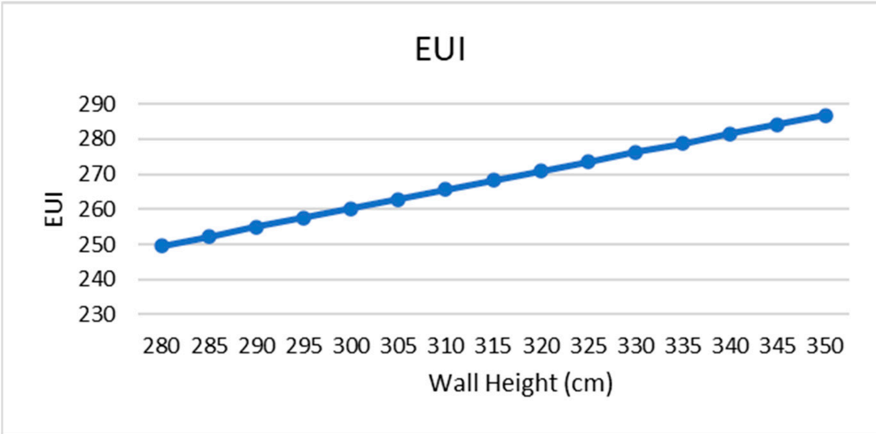


**Figure 21.** The linear relation between EUI and wall height.

**Table 9.** The EUI results for different wall height.

| Wall Height (cm) | 280 | 285 | 290 | 295 | 300 | 305 | 310 | 315 | 320 | 325 | 330 | 335 | 340 | 345 | 350 |
|---|---|---|---|---|---|---|---|---|---|---|---|---|---|---|---|
| EUI, kWh/m$^2$ | 249.53 | 252.36 | 254.87 | 257.54 | 260.21 | 262.826 | 265.55 | 268.166 | 270.836 | 273.507 | 276.229 | 278.792 | 281.516 | 284.186 | 286.802 |
| Enhancement ration | 38.8% | 38.1% | 37.5% | 36.8% | 36.2% | 35.5% | 34.9% | 34.2% | 33.6% | 32.9% | 32.2% | 31.6% | 31.0% | 30.3% | 29.7% |

The mathematical model can be defined as Equation (3), where EUI is the energy use intensity and WH is the wall height. The equation is made according to the previous data, which shows the EUI results for different wall heights. A linear relationship between the wall height and EUI has been observed. The fit residual between Equation (3) and the real values of EUI is between −0.05 and 0.12, as seen in Figure 22.

$$EUI = 100.91 + 0.532\ WH \tag{3}$$

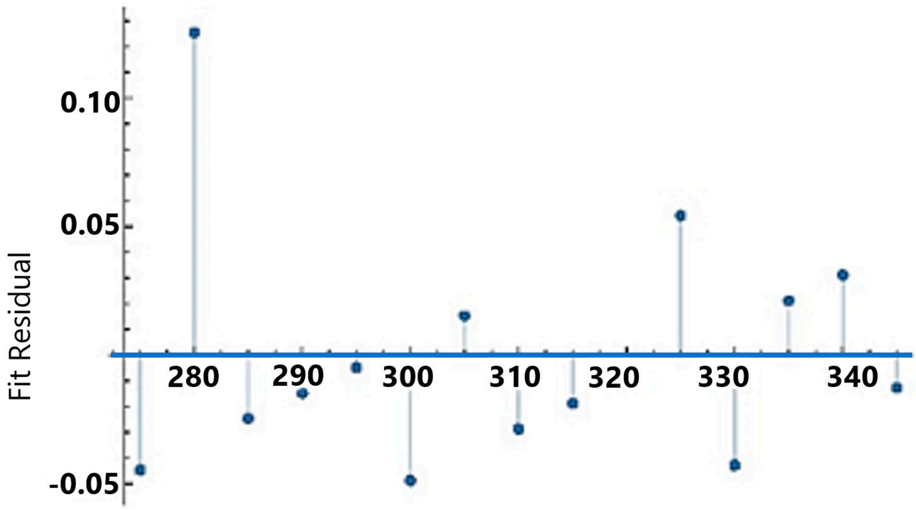


**Figure 22.** The residual fit between the equations.

### *3.5. Applying the Optimum Wall Design in Jazan City*

Following the optimization of the wall section, the study extended its investigation to Jazan City, Saudi Arabia, aiming to assess the applicability of the developed method in similar climatic regions. The study specifically targeted Jazan City to elucidate the disparities among the three investigated cases: (1) the base case; (2) the wall incorporating the brick with the most favorable waste ratio; and (3) the optimized wall section.

In terms of thermal performance, the research focused on simulating two key metrics: thermal comfort and energy consumption for Jazan. Thermal comfort was assessed using two metrics: PMV and PPD. The study utilized these thermal comfort indices to identify the best-performing wall section and compared the results with those of the base case. Subsequently, the study simulated the total EUI and energy balance. Additionally, monthly heating and cooling loads were simulated for both the optimal wall section and the base case.

#### 3.5.1. Thermal Comfort for Jazan City

The analysis of thermal comfort in Jazan, presented in Table 10, indicates a discernible trend, showcasing noteworthy enhancements in both PMV and PPD. Particularly, employing the optimized wall section, as recommended by the optimization process, demonstrates further improvements compared to using bricks with 15% of waste alone. This underscores the significant contribution of the optimized wall section to enhancing thermal comfort, consistent with the findings observed in the investigated case study building in Egypt.

**Table 10.** Thermal comfort for Jazan for base case, 15% of waste, and optimum wall section.

| | | PMV | | PPD |
|---|---|---|---|---|
| Base case | | 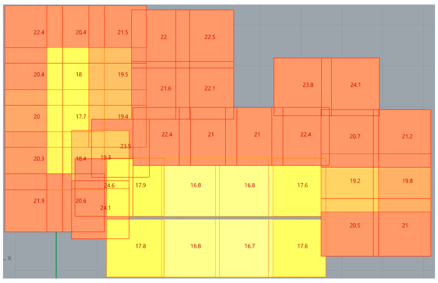 | | 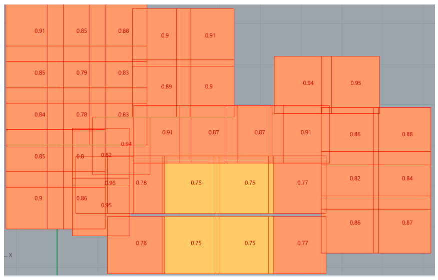 |
| 15% Waste ratio | 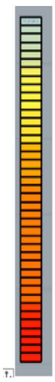 | 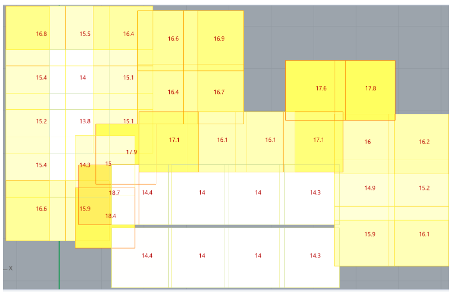 |  | 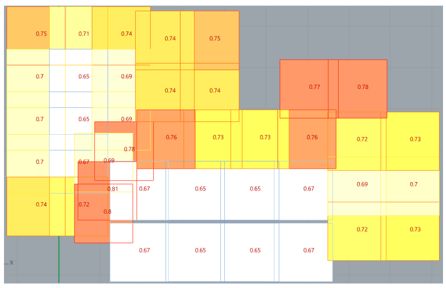 |
| Optimum wall section | | 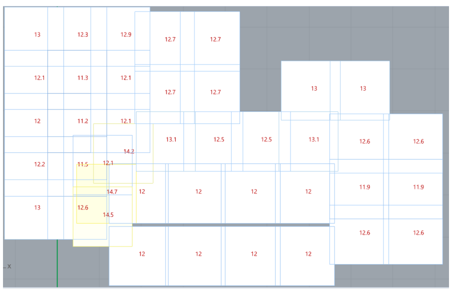 | | 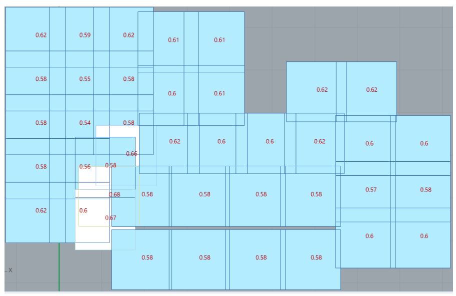 |

### 3.5.2. $CO_2$ Reduction for Jazan City

Through an analysis of $CO_2$ emissions from the investigated building in Jazan, this study revealed a clear, inversely proportional relationship that became increasingly pronounced with higher waste ratios in the fabricated brick. Specifically, the brick containing 15% of waste showed a notable reduction of nearly 13% in $CO_2$ emissions compared to the base case. Furthermore, the implementation of the optimized wall section further intensified this reduction, reaching approximately 25%. These findings highlight the significant potential of incorporating waste materials and sustainable design practices to promote environmental sustainability. Such initiatives align with the global imperative to mitigate carbon footprints in construction practices, as illustrated in Figure 23a,b.

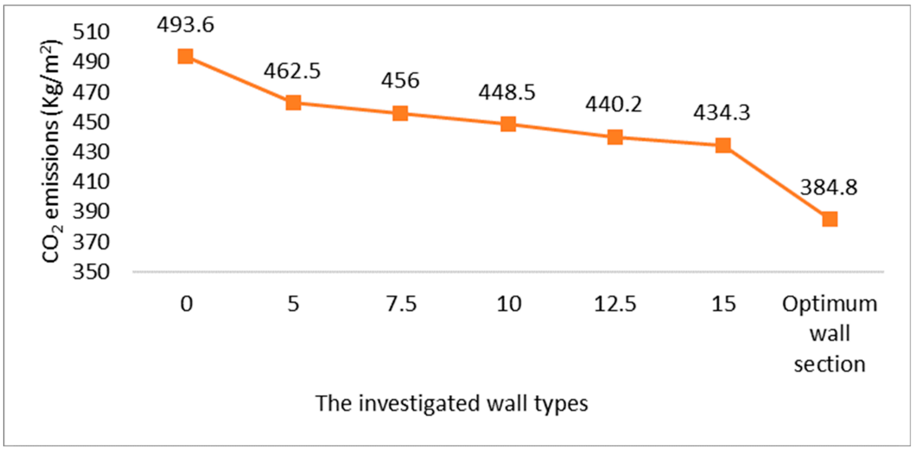


(**a**)

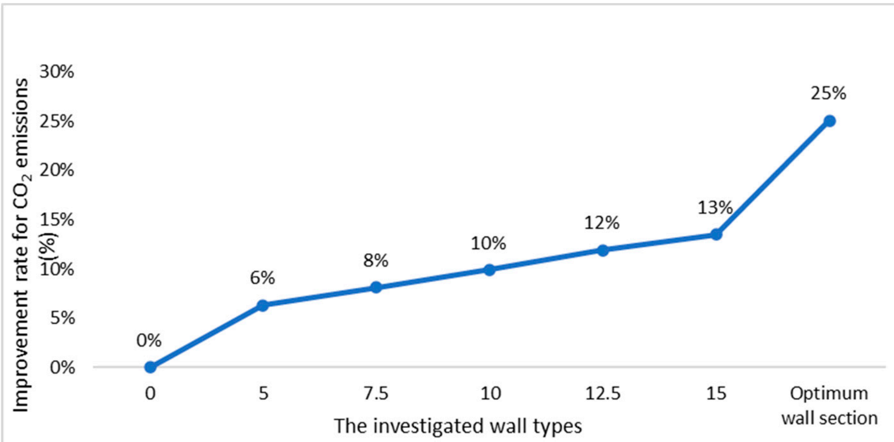


(**b**)

**Figure 23.** $CO_2$ emissions: (**a**) the amount of $CO_2$ emissions, (**b**) the improvement rate in terms of $CO_2$ reduction%.

### 3.5.3. EUI, Cooling, and Heating Loads

The results pertaining to cooling loads in Jazan, as presented in Figure 24 and Table 11, reveal a notable trend, suggesting substantial improvements. Notably, employing the optimized wall section, as advised by the optimization process, yields even more pronounced enhancements, showing a 41% improvement compared to using bricks with 15% of waste alone.

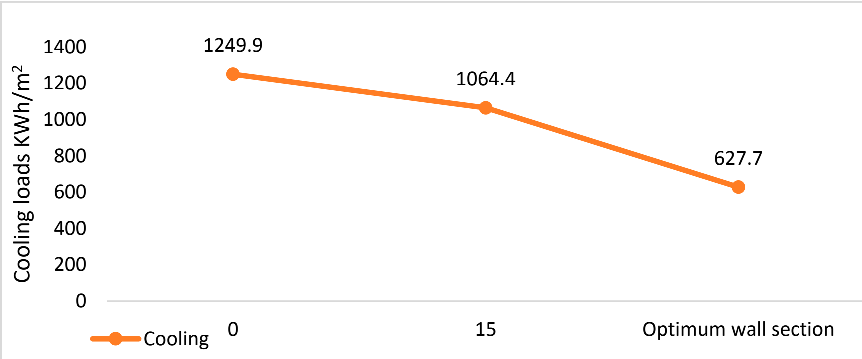


**Figure 24.** Cooling loads for Jazan City.

**Table 11.** Cooling loads for the three approaches in Jazan.

| | 0% | 15% | Optimum |
|---|---|---|---|
| Bathroom | 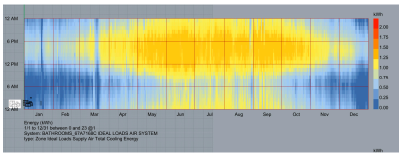 | 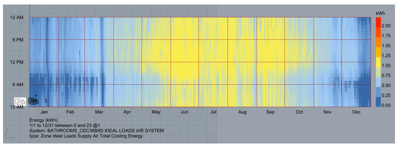 | 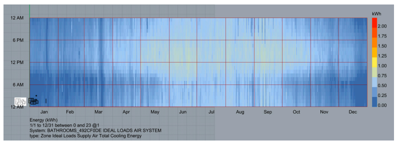 |
| Bedroom | 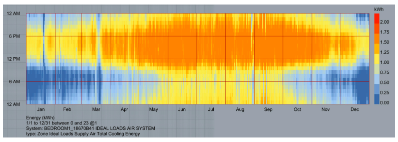 | 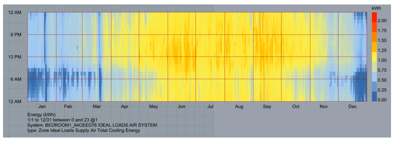 | 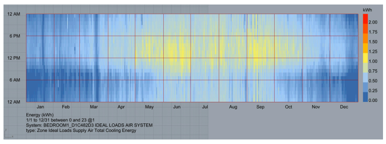 |
| Bedroom2 | 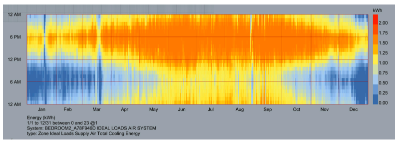 | 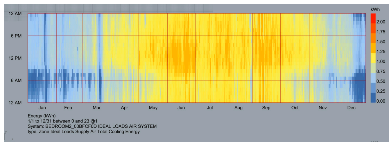 | 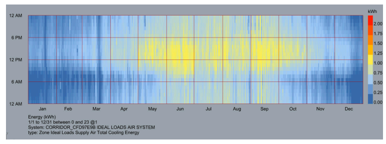 |
| Corridor | 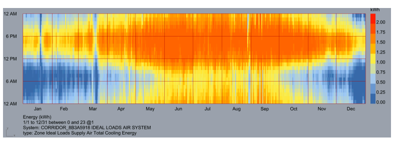 | 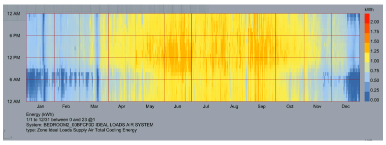 | 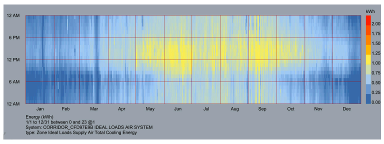 |
| Kitchen | 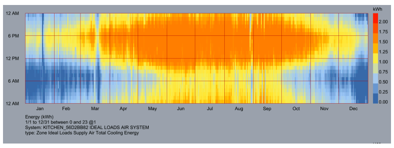 | 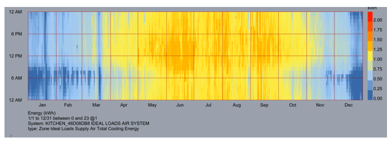 | 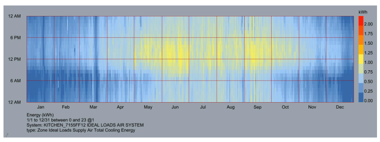 |
| Master Bedroom | 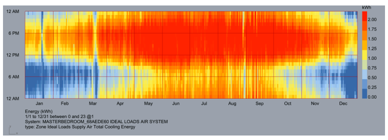 | 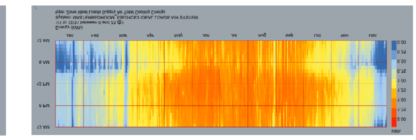 | 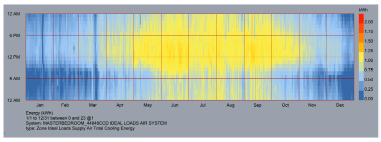 |
| Reception | 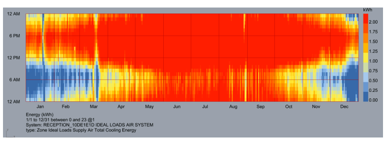 | 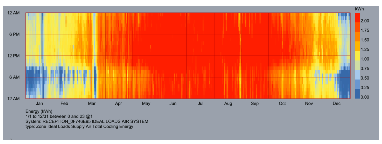 | 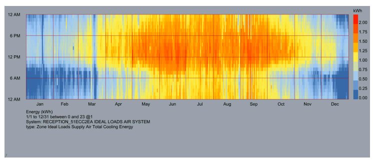 |

## 4. Discussion

The selected case study, representing a high-rise social housing building in New Cairo, provides valuable insights into the thermal performance of multi-story residential constructions. The study focuses specifically on simulating the southwest apartment, anticipating the highest heat gain in this area. The primary objective is to investigate how waste ratios affect thermal comfort and energy consumption in residential buildings. This comprehensive approach aims to minimize heating and cooling energy demand while enhancing thermal comfort in investigated rooms, thereby contributing to overall energy reduction in high-rise residential structures. The evaluation process is enhanced by integrating Honeybee, Daysim, Open Studio, and EnergyPlus for energy load simulations, utilizing metrics such as EUI, heating and cooling loads, and energy balance to quantify energy performance. Parametric design techniques and genetic optimization strategies were employed to enhance the thermal performance of the building envelope, resulting in improved thermal comfort across various waste ratios.

The incorporation of 15% of *Pleurotus florida* waste in the brick composition yielded the most significant enhancement, leading to a notable 17% reduction in EUI. Notably, the study reveals a direct relationship between energy balance and waste ratio, providing valuable insights into sustainable construction practices. The investigation into thermal comfort identifies a noteworthy pattern, with promising enhancements observed in both the PMV and PPD metrics. The gradual improvement in thermal comfort, peaking at a 15% waste ratio, highlights a proportional link between waste ratio and improved indoor environmental conditions. This finding aligns with the principles of thermal insulation and energy efficiency, suggesting opportunities for architects and builders to optimize indoor thermal conditions effectively. Furthermore, the simulation results for EUI demonstrate a systematic decrease with increasing waste ratios in the bricks, positively influencing energy balance, cooling, and heating loads.

Environmental impact assessment reveals an inversely proportional relationship between waste ratio and $CO_2$ emissions, notably evident in the brick containing 15% of waste, which exhibits a significant reduction of nearly 6% compared to the base case. This underscores the potential of waste materials to contribute to environmental sustainability, aligning with global efforts to mitigate carbon footprints in construction practices.

The optimization process, spanning six cases, indicates that energy efficiency reaches its optimal solution starting in the third case. The results emphasize the pronounced impact of gap thickness compared to brick thickness, with greater gap thickness consistently yielding improved performance. Optimal wall sections feature maximum wall brick thickness and substantial gap thickness, highlighting the critical role of gap thickness in enhancing overall energy efficiency. Additionally, the optimization process identifies height as a significant determinant of EUI, leading to the determination of optimal wall heights ranging from 280 cm to 285 cm. These findings underscore a notable correlation between height and EUI. The mathematical equation correlating building height and EUI, derived through initial model development and processing using "Mathematica 10" software, provides architects with a tool to tailor building heights according to specific energy use intensity requirements. The equation's flexibility allows for adjustments and refinements using various techniques, ensuring adaptability to a broader range of scenarios. Furthermore, the study proposes a novel wall design utilizing optimal bricks and employs a genetic algorithm to optimize its thickness and height, resulting in a remarkable 38.7% reduction in EUI compared to the base case.

## 5. Conclusions

In this study, the effects of varying heating parameters on the properties of fired clay bricks were investigated. The experiments involved heating the brick samples to temperatures ranging from 700 °C to 900 °C, with different heating rates and target temperatures. Based on the obtained results, the following conclusions can be drawn:

- In terms of mechanical properties, the compressive strength of fired clay bricks was observed to decrease with higher levels of *Pleurotus florida* waste content and improve with increasing firing temperature, indicating that a smaller amount of *Pleurotus florida* waste and higher firing temperatures can enhance the bricks' compressive strength.
- Regarding physical properties, the bulk density of fired clay bricks exhibited a decrease with higher levels of *Pleurotus florida* waste content, while it increased with firing temperature. This implies that increasing the *Pleurotus florida* waste content reduces the overall density of the bricks, whereas higher firing temperatures lead to denser bricks. Similarly, the apparent porosity of fired clay bricks showed an increase with higher levels of *Pleurotus florida* waste content and a decrease as firing temperature increased, indicating a denser structure resulting from incorporating less *Pleurotus florida* waste and subjecting the bricks to higher firing temperatures.
- The study also revealed that bricks containing *Pleurotus florida* waste demonstrated lower thermal conductivity compared to conventional bricks, making them more energy-efficient. For instance, using 15% of *Pleurotus florida* waste resulted in a significant 61.94% reduction in thermal conductivity compared to conventional bricks. Moreover, bricks with *Pleurotus florida* waste were found to enhance indoor thermal comfort, with an optimal waste ratio of 15%.
- The energy performance of the building was evaluated, the results showed that bricks with higher waste ratios led to greater energy savings. For example, the brick with a waste ratio of 5% achieved a 6% energy saving, while the brick with 15% waste demonstrated the best energy saving of 17%. Furthermore, bricks with higher waste ratios exhibited lower $CO_2$ emissions, with a nearly 6% reduction in $CO_2$ emissions compared to the base case with no incorporated waste.

This study underscores the significant potential of incorporating *Pleurotus florida* waste into clay bricks to improve thermal performance and decrease energy use intensity (EUI). Notably, the optimized design featuring an air gap between bricks showcases the paramount influence of design parameters on material efficiency and EUI. The best wall section achieved an impressive 38.7% reduction in EUI, highlighting the substantial impact of this innovative approach on energy efficiency in construction. In essence, this study bridges the gap between sustainable material incorporation, thermal performance improvement, and optimized architectural design. The findings provide a blueprint for architects and construction engineers to leverage waste-derived bricks and innovative design strategies to create energy-efficient structures without compromising performance or material integrity. Ultimately, this research paves the way for greener, more sustainable construction practices that prioritize both environmental consciousness and energy efficiency. To conclude, the study provides valuable insights into the relationship between mechanical and physical properties of fired clay bricks, highlighting the effects of *Pleurotus florida* waste content and firing temperature. Additionally, it demonstrates the energy efficiency and thermal comfort benefits of incorporating florida waste into brick production, emphasizing the potential for reducing $CO_2$ emissions.

**Author Contributions:** Conceptualization, M.K.F. and D.T.; methodology, M.K.F. and A.R.; software, M.K.F. and A.R.; formal analysis, A.Y. and I.M.M.; investigation, M.M.A. and S.A.A.; resources, A.Y. and I.M.M.; data curation, M.K.F. and D.T.; writing—original draft preparation, M.M.A. and M.K.F.; writing—review and editing, A.R. and S.A.A.; visualization, M.K.F. and A.R.; project administration, I.M.M. and A.Y.; funding acquisition, I.M.M. and A.Y. All authors have read and agreed to the published version of the manuscript.

**Funding:** The research was funded by the Deputyship for Research and Innovation, Ministry of Education in Saudi Arabia through project number ISP23-58.

**Data Availability Statement:** Data is contained within the article.

**Acknowledgments:** The authors extend their appreciation to the Deputyship for Research & Innovation, Ministry of Education in Saudi Arabia, for funding this research work through project number ISP23-58.

**Conflicts of Interest:** The authors declare no conflicts of interest.

## References


1. Khani, A.; Khakzand, M.; Faizi, M. Multi-objective optimization for energy consumption, visual and thermal comfort performance of educational building (case study: Qeshm Island, Iran). *Sustain. Energy Technol. Assess.* **2022**, *54*, 102872. [CrossRef]
2. Delgarm, N.; Sajadi, B.; Delgarm, S.; Kowsary, F. A novel approach for the simulation-based optimization of the buildings energy consumption using NSGA-II: Case study in Iran. *Energy Build.* **2016**, *127*, 552–560. [CrossRef]
3. Rizi, R.A.; Eltaweel, A. A user detective adaptive facade towards improving visual and thermal comfort. *J. Build. Eng.* **2021**, *33*, 101554. [CrossRef]
4. Eze, V.H.U.; Tamball, J.S.; Uzoma, O.F.; Sarah, N.I.; Robert, O.; Wisdom, O.O. Advancements in Energy Efficiency Technologies for Thermal Systems: A Comprehensive Review. *INOSR Appl. Sci.* **2024**, *12*, 1–20. [CrossRef]
5. Abd Elrady, A.; Hassan, M. Conservation of morphological characters as an approach to thermal comfort. In *Vernacular Architecture: Towards a Sustainable Future*; CRC Press: London, UK, 2015; p. 15. [CrossRef]
6. Mamajonova, N.; Oydin, M.; Usmonali, T.; Olimjon, A.; Madina, A.; Marguba, M. Parametric Design: Enhancing Architectural Environments through Computational Innovatio. *Hold. Reason.* **2024**, *2*, 334–345.
7. González-Torres, M.; Pérez-Lombard, L.; Coronel, J.F.; Maestre, I.R.; Yan, D. A review on buildings energy information: Trends, end-uses, fuels and drivers. *Energy Rep.* **2022**, *8*, 626–637. [CrossRef]
8. Labaran, Y.H.; Mathur, V.S.; Muhammad, S.U.; Musa, A.A. Carbon footprint management: A review of construction industry. *Clean. Eng. Technol.* **2022**, *9*, 100531. [CrossRef]
9. Tsay, Y.-S.; Yeh, Y.-C.; Jheng, H.-Y. Study of the tools used for early-stage carbon footprint in building design. *e-Prime-Adv. Electr. Eng. Electron. Energy* **2023**, *4*, 100128. [CrossRef]
10. Tarek, N.; Aly, A.M.M.; Ragab, A. Energy-Efficient Passive Cooling Design for Residential Buildings in Hot and Arid Climates: A Parametric Study. *Aswan Univ. J. Sci. Technol.* **2024**, *4*, 80–95. [CrossRef]
11. Mahmoud, A.R. Investigating the Impact of Different Glazing Types on the Energy Performance in Hot Arid Climate. *J. Adv. Eng. Trends* **2022**, *42*, 69–84. [CrossRef]
12. Abdelrady, A.; Abdelhafez, M.H.H.; Ragab, A. Use of insulation based on nanomaterials to improve energy efficiency of residential buildings in a hot desert climate. *Sustainability* **2021**, *13*, 5266. [CrossRef]
13. Langbehn, R.K.; Michels, C.; Soares, H.M. Antibiotics in wastewater: From its occurrence to the biological removal by environmentally conscious technologies. *Environ. Pollut.* **2021**, *275*, 116603. [CrossRef] [PubMed]
14. Miao, Y.; Ye, T.; Xiao, J.; Lau, S.S.Y.; Zhou, Z. Investigation on alkali-activated insulation mortar containing high-volume recycled concrete powder for energy-efficient buildings. *Energy Build.* **2024**, *303*, 113825. [CrossRef]
15. Liu, B.; Wang, Y.; Rabczuk, T.; Olofsson, T.; Lu, W. Multi-scale modeling in thermal conductivity of Polyurethane incorporated with Phase Change Materials using Physics-Informed Neural Networks. *Renew. Energy* **2024**, *220*, 119565. [CrossRef]
16. Nasri, W.; Djebali, R.; Chamkha, A.J.; Bezazi, A.; Mechighel, F.; Reis, P.; Driss, Z. Thermal behavior of mesoporous Aramid fiber reinforced silica aerogel composite for thermal insulation applications: Microscale modeling. *J. Appl. Comput. Mech.* **2024**, *10*, 140–151.
17. Rashad, A.M.; Mosleh, Y.A.; Mokhtar, M. Thermal insulation and durability of alkali-activated lightweight slag mortar modified with silica fume and fly ash. *Constr. Build. Mater.* **2024**, *411*, 134255. [CrossRef]
18. Mezaien, A.; Baltazar, J.-C. Evaluating the Performance of a Passive Architectural Element in a Hot-Dry Climate Through Natural Ventilation and Thermal Impact Analysis. In Proceedings of the American Solar Energy Society National Conference, Boulder, CO, USA, 8–11 August 2023; pp. 171–183.
19. Cantor, D.M.; Manea, D.L. Innovative building materials using agricultural waste. *Procedia Technol.* **2015**, *19*, 456–462.
20. Zeyad, A.M. Sustainable concrete Production: Incorporating recycled wastewater as a green building material. *Constr. Build. Mater.* **2023**, *407*, 133522. [CrossRef]
21. Zeyad, A.M.; Magbool, H.M.; Tayeh, B.A.; de Azevedo, A.R.G.; Abutaleb, A.; Hussain, Q. Production of geopolymer concrete by utilizing volcanic pumice dust. *Case Stud. Constr. Mater.* **2022**, *16*, e00802. [CrossRef]
22. Zeyad, A.M.; Johari, M.A.M.; Abadel, A.; Abutaleb, A.; Mijarsh, M.; Almalki, A. Transport properties of palm oil fuel ash-based high-performance green concrete subjected to steam curing regimes. *Case Stud. Constr. Mater.* **2022**, *16*, e01077. [CrossRef]
23. Zeyad, A.M.; Shubaili, M.; Abutaleb, A. Using volcanic pumice dust to produce high-strength self-curing concrete in hot weather regions. *Case Stud. Constr. Mater.* **2023**, *18*, e01927. [CrossRef]
24. Korpayev, S.; Bayramov, M.; Durdyev, S.; Hamrayev, H.; Baymyradova, D.; Nurmuhammedov, A. Effect of stone wool waste from greenhouse agriculture in brick production. *J. Build. Eng.* **2023**, *63*, 105340. [CrossRef]
25. Hassan, A.M.S.; Abdeen, A.; Mohamed, A.S.; Elboshy, B. Thermal performance analysis of clay brick mixed with sludge and agriculture waste. *Constr. Build. Mater.* **2022**, *344*, 128267. [CrossRef]
26. Ya-bin, C.; Xing-wang, P.; Bing-zheng, H. Thermal performance analysis of building construction with insulated walls in summer days and nights. *J. Cent. South Univ.* **2021**, *28*, 3613–3625.
27. Ravelo, B.; Rajaoarisoa, L.; Maurice, O. Thermal modelling of multilayer walls for building retrofitting applications. *J. Build. Eng.* **2020**, *29*, 101126. [CrossRef]
28. François, A.; Ibos, L.; Feuillet, V.; Meulemans, J. Estimation of the thermal resistance of a building wall with inverse techniques based on rapid active in situ measurements and white-box or ARX black-box models. *Energy Build.* **2020**, *226*, 110346. [CrossRef]

29. Flores-Ales, V.; Alducin-Ochoa, J.M.; Martín-del-Río, J.J.; Torres-Gonzalez, M.; Jimenez-Bayarri, V. Physical-mechanical behaviour and transformations at high temperature in a cement mortar with waste glass as aggregate. *J. Build. Eng.* **2020**, *29*, 101158. [CrossRef]
30. Al-Sanea, S.A.; Zedan, M. Improving thermal performance of building walls by optimizing insulation layer distribution and thickness for same thermal mass. *Appl. Energy* **2011**, *88*, 3113–3124. [CrossRef]
31. Ahmed, S.; El Attar, M.E.; Zouli, N.; Abutaleb, A.; Maafa, I.M.; Ahmed, M.; Yousef, A.; Ragab, A. Improving the Thermal Performance and Energy Efficiency of Buildings by Incorporating Biomass Waste into Clay Bricks. *Materials* **2023**, *16*, 2893. [CrossRef]
32. Ragab, A.; Zouli, N.; Abutaleb, A.; Maafa, I.M.; Ahmed, M.; Yousef, A. Environmental and Economic Benefits of Using Pomegranate Peel Waste for Insulation Bricks. *Materials* **2023**, *16*, 5372. [CrossRef]
33. Xie, X.; Zhang, W.; Luan, X.; Gao, W.; Geng, X.; Xue, Y. Thermal performance enhancement of hollow brick by agricultural wastes. *Case Stud. Constr. Mater.* **2022**, *16*, e01047. [CrossRef]
34. Sangmesh, B.; Patil, N.; Jaiswal, K.K.; Gowrishankar, T.; Selvakumar, K.K.; Jyothi, M.; Jyothilakshmi, R.; Kumar, S. Development of sustainable alternative materials for the construction of green buildings using agricultural residues: A review. *Constr. Build. Mater.* **2023**, *368*, 130457.
35. Khalil, A.; Tolba, O.; Ezzeldin, S. Optimization of an office building form using a lattice incubate boxes method. *Adv. Eng. Inform.* **2023**, *55*, 101847. [CrossRef]
36. Jasińska, A. Spent mushroom compost (SMC)–retrieved added value product closing loop in agricultural production. *Acta Agrar. Debreceniensis* **2018**, *150*, 185–202. [CrossRef]
37. Bakmohammadi, P.; Noorzai, E. Optimization of the design of the primary school classrooms in terms of energy and daylight performance considering occupants' thermal and visual comfort. *Energy Rep.* **2020**, *6*, 1590–1607. [CrossRef]
38. Singh, A.D.; Vikineswary, S.; Abdullah, N.; Sekaran, M. Enzymes from spent mushroom substrate of Pleurotus sajor-caju for the decolourisation and detoxification of textile dyes. *World J. Microbiol. Biotechnol.* **2011**, *27*, 535–545. [CrossRef]
39. Jones, M.; Mautner, A.; Luenco, S.; Bismarck, A.; John, S. Engineered mycelium composite construction materials from fungal biorefineries: A critical review. *Mater. Des.* **2020**, *187*, 108397. [CrossRef]
40. Holt, G.A.; Mcintyre, G.; Flagg, D.; Bayer, E.; Wanjura, J.; Pelletier, M. Fungal mycelium and cotton plant materials in the manufacture of biodegradable molded packaging material: Evaluation study of select blends of cotton byproducts. *J. Biobased Mater. Bioenergy* **2012**, *6*, 431–439. [CrossRef]
41. Yang, Z.; Zhang, F.; Still, B.; White, M.; Amstislavski, P. Physical and mechanical properties of fungal mycelium-based biofoam. *J. Mater. Civ. Eng.* **2017**, *29*, 04017030. [CrossRef]
42. Xing, Y.; Brewer, M.; El-Gharabawy, H.; Griffith, G.; Jones, P. Growing and testing mycelium bricks as building insulation materials. In *IOP Conference Series: Earth and Environmental Science*; IOP Publishing: Bristol, UK, 2018; p. 022032.
43. Wimmers, G.; Klick, J.; Tackaberry, L.; Zwiesigk, C.; Egger, K.; Massicotte, H. Fundamental studies for designing insulation panels from wood shavings and filamentous fungi. *BioResources* **2019**, *14*, 5506–5520. [CrossRef]
44. Satbaev, B.; Yefremova, S.; Zharmenov, A.; Kablanbekov, A.; Yermishin, S.; Shalabaev, N.; Satbaev, A.; Khen, V. Rice husk research: From environmental pollutant to a promising source of organo-mineral raw materials. *Materials* **2021**, *14*, 4119. [CrossRef] [PubMed]
45. Grimm, D.; Wösten, H.A. Mushroom cultivation in the circular economy. *Appl. Microbiol. Biotechnol.* **2018**, *102*, 7795–7803. [CrossRef] [PubMed]
46. Phan, C.-W.; Sabaratnam, V. Potential uses of spent mushroom substrate and its associated lignocellulosic enzymes. *Appl. Microbiol. Biotechnol.* **2012**, *96*, 863–873. [CrossRef] [PubMed]
47. Jabi, W. *Parametric Design for Architecture*; Hachette: London, UK, 2013.
48. Eltaweel, A.; Yuehong, S. Parametric design and daylighting: A literature review. *Renew. Sustain. Energy Rev.* **2017**, *73*, 1086–1103. [CrossRef]
49. Fahmy, M.K. Applying Urban Parametricism in the Design of Dynamic Neighborhoods. In Transformations and Challenges [9th ASCAAD Conference Proceedings ISBN 978-1-907349-20-1] Cairo (Egypt), Virtual Conference. pp. 2–4. Available online: https://papers.cumincad.org/cgi-bin/works/paper/ascaad2021_028 (accessed on 27 December 2023).
50. Fahmy, M.K.; Eltaweel, A.; Rizi, R.A.; Imani, N. Integrated Kinetic Fins for Western Facades in Territories with Low Solar Altitudes. *Buildings* **2023**, *13*, 782. [CrossRef]
51. Okigbo, R.; Muonyelu, N.; Egwu, A. Effect of using rice husk for cultivation of *Pleurotus tuberregium* (FR.) SINGER. *J. Basic Appl. Res. Int.* **2021**, *27*, 1–10.
52. Al-Jabri, K.; Shoukry, H.; Mokhtar, M.M.; Morsy, M.S. Thermo-physical, mechanical and microstructural properties of cementless lightweight mortar. *Adv. Cem. Res.* **2021**, *33*, 74–83. [CrossRef]
53. Phonphuak, N. Application of dry grass for clay brick manufacturing. *Key Eng. Mater.* **2017**, *757*, 35–39. [CrossRef]
54. Gencel, O.; Munir, M.J.; Kazmi, S.M.S.; Sutcu, M.; Erdogmus, E.; Velasco, P.M.; Quesada, D.E. Recycling industrial slags in production of fired clay bricks for sustainable manufacturing. *Ceram. Int.* **2021**, *47*, 30425–30438. [CrossRef]
55. *ASTM: D5334-08*; Standard Test Method for Determination of Thermal Conductivity of Soil Soft Rock by Thermal Needle Probe Procedure. ASTM International: West Conshohocken, PA, USA, 2008.

56. Chen, R.; Tsay, Y.-S. Carbon emission and thermal comfort prediction model for an office building considering the contribution rate of design parameters. *Energy Rep.* **2022**, *8*, 8093–8107. [CrossRef]
57. Zou, Y.; Zhan, Q.; Xiang, K. A comprehensive method for optimizing the design of a regular architectural space to improve building performance. *Energy Rep.* **2021**, *7*, 981–996. [CrossRef]
58. Ministry of Housing and Works, Government of Pakistan Lahore. *Building Code of Pakistan—Seismic Hazard Evaluation Studies*; Ministry of Housing and Works, Government of Pakistan Lahore: Islamabad, Pakistan, 2007.
59. Bureau of Indian Standards (BIS). *Specifications for Common Burnt Clay Building Bricks*; 5th Revision; IS: 3495 (Part-I to IV); BIS: New Delhi, India, 1992.
60. *NBR-6064*; Ceramic soft-mud brick—Assessment of compressive strength—Assay method. Brazilian Association of Technical Standards (ABNT): Rio de Janeiro, Brazil, 1983.
61. *IS1077-1992*; Common Burnt Clay Building Bricks-Specification. Bureau of Indian Standards, N.D.: New Delhi, India, 2007. Available online: https://law.resource.org/pub/in/bis/S03/is.1077.1992.pdf (accessed on 27 December 2023).
62. *CNS382-R2002*; Building with Ordinary Brick. National Standard Republic of China: Beijing, China, 2002. Available online: https://www.confinedmasonry.org/wp-content/uploads/2009/09/China_Code_seismic_design_buildings.pdf (accessed on 27 December 2023).
63. *ES4763*; Building of Brick Masonry Units Made from Clay. Egyptian Organization for Standardization & Quality: Cario, Egypt, 2006. Available online: https://law.resource.org/pub/eg/ibr/es.4763.2006.pdf (accessed on 27 December 2023).
64. *ASTM C62*; Standard Specification for Building Brick (Solid Masonry Units Made from Clay or Shale). ASTM: Philadelphia, PA, USA, 2012. Available online: http://www.masonryinstitute.com/wp-content/uploads/ASTM_C216-10.pdf (accessed on 27 December 2023).
65. *ASTM C90*; Standard Specification for Loadbearing Concrete Masonry Units. ASTM: Philadelphia, PA, USA, 2014. Available online: https://spectraglaze.com/wp-content/uploads/2018/04/ASTM-C90-122117.pdf (accessed on 27 December 2023).
66. Maza-Ignacio, O.T.; Jiménez-Quero, V.G.; Guerrero-Paz, J.; Montes-García, P. Recycling untreated sugarcane bagasse ash and industrial wastes for the preparation of resistant, lightweight and ecological fired bricks. *Constr. Build. Mater.* **2020**, *234*, 117314. [CrossRef]
67. Ölmez, H.; Erdem, E. The effects of phosphogypsum on the setting and mechanical properties of Portland cement and trass cement. *Cem. Concr. Res.* **1989**, *19*, 377–384. [CrossRef]
68. Rashad, A.M.; Gharieb, M.; Shoukry, H.; Mokhtar, M.M. Valorization of sugar beet waste as a foaming agent for metakaolin geopolymer activated with phosphoric acid. *Constr. Build. Mater.* **2022**, *344*, 128240. [CrossRef]